Hyperscaling violation at the Ising-nematic quantum critical point in two-dimensional metals

Permanent link

Terms of Use

Share Your Story

Hyperscaling violation at the Ising-nematic quantum critical point in two dimensional metals

Andreas Eberlein,[1] Ipsita Mandal,[2] and Subir Sachdev[1,2]

[1]*Department of Physics, Harvard University, Cambridge MA 02138, USA*
[2]*Perimeter Institute for Theoretical Physics,*
Waterloo, Ontario, Canada N2L 2Y5

(Dated: May 4, 2016)

Abstract

Understanding optical conductivity data in the optimally doped cuprates in the framework of quantum criticality requires a strongly-coupled quantum critical metal which violates hyperscaling. In the simplest scaling framework, hyperscaling violation can be characterized by a single non-zero exponent θ, so that in a spatially isotropic state in d spatial dimensions, the specific heat scales with temperature as $T^{(d-\theta)/z}$, and the optical conductivity scales with frequency as $\omega^{(d-\theta-2)/z}$ for $\omega \gg T$, where z is the dynamic critical exponent. We study the Ising-nematic critical point, using the controlled dimensional regularization method proposed by Dalidovich and Lee (Phys. Rev. B **88**, 245106 (2013)). We find that hyperscaling is violated, with $\theta = 1$ in $d = 2$. We expect that similar results apply to Fermi surfaces coupled to gauge fields in $d = 2$.

CONTENTS

I. INTRODUCTION

The widespread observation of 'strange metal' behavior in numerous correlated electron compounds underscores the need for a general theoretical framework for understanding metallic states without quasiparticle excitations [1]. Theories of such metallic states involve fermionic excitations across a Fermi surface coupled to low energy and long-wavelength excitations of some gapless boson. This boson can either be a symmetry-breaking order parameter at a critical point [2–10], an emergent deconfined gauge field [6, 11–15], and/or a critical 'Higgs' field associated with phase transition between different phases of a gauge theory [16, 17]. In all of these cases, the critical theory of the non-quasiparticle metal can be formulated as a continuum theory with an exactly conserved momentum density $\boldsymbol{P}$ [17–19]. The other conserved quantities in such theories are the fermion number density and the energy density.

Such a continuum theory can provide a reliable computation for numerous single particle and other non-transport response functions. However, the conservation of $\boldsymbol{P}$ leads to singularities in the transport properties which have to be regulated by various "lattice" contributions. Umklapp scattering and/or impurities are needed to dissipate the momentum, and to obtain finite transport co-efficients in the d.c. limit. At frequencies $\omega > T$, e.g. in the optical conductivity of interest in the present paper, the effects of $\boldsymbol{P}$ are less important; nevertheless, it is important to subtract out the singular contributions in the d.c. limit to properly define the scaling properties of frequency-dependent transport co-efficients. In a number of recent papers, 'memory function', hydrodynamic, and holographic methods have been employed to understand the lattice contributions to the low frequency transport [20–26].

For our purposes, it is useful to describe the transport properties in the limit where $\boldsymbol{P}$ is exactly conserved. Then the thermoelectric response is described by

$$\begin{pmatrix} \boldsymbol{J} \\ \boldsymbol{Q} \end{pmatrix} = \begin{pmatrix} \sigma & \alpha \\ T\alpha & \overline{\kappa} \end{pmatrix} \begin{pmatrix} \boldsymbol{E} \\ -\boldsymbol{\nabla}T \end{pmatrix}, \tag{1.1}$$

where T is temperature, $\boldsymbol{E}$ is an applied electric field, $\boldsymbol{J}$ is the electrical current, and $\mathbf{Q}$ is the heat current. The electrical conductivity, σ, and thermoelectric conductivities $\alpha, \overline{\kappa}$, are in general spatial matrices, but we will only consider here spatially isotropic systems without an external magnetic field, and then these conductivities are numbers. The thermal conductivity, κ, is defined under conditions under which $\boldsymbol{J} = 0$, and so

$$\kappa = \overline{\kappa} - \frac{T\alpha^2}{\sigma}. \tag{1.2}$$

In systems with $\boldsymbol{P}$ conserved, the thermoelectric conductivities have poles at zero frequency, ω,

and obey [25]

$$\sigma = \frac{\mathcal{Q}^2}{\mathcal{M}} \left(\frac{1}{-i\omega} \right) + \sigma_Q$$

$$\alpha = \frac{\mathcal{S}\mathcal{Q}}{\mathcal{M}} \left(\frac{1}{-i\omega} \right) + \alpha_Q$$

$$\overline{\kappa} = \frac{T\mathcal{S}^2}{\mathcal{M}} \left(\frac{1}{-i\omega} \right) + \overline{\kappa}_Q, \tag{1.3}$$

where σ_Q, α_Q, $\overline{\kappa}_Q$ are the frequency-dependent conductivities after the pole has been subtracted out. The residues of the pole are related exactly to static thermodynamic observables: these are the entropy density, $\mathcal{S}$, the current-momentum correlator $\mathcal{Q} \equiv \chi_{J_x,P_x}$, and the momentum-momentum correlator $\mathcal{M} \equiv \chi_{P_x,P_x}$. Combining Eqs. (1.2) and (1.3), we observe that the pole at $\omega = 0$ does not appear in κ, and in the d.c. limit [20, 27]

$$\kappa = \overline{\kappa}_Q - 2 \left(\frac{T\mathcal{S}}{\mathcal{Q}} \right) \alpha_Q + \left(\frac{T\mathcal{S}^2}{\mathcal{Q}^2} \right) \sigma_Q \quad , \quad \omega \to 0. \tag{1.4}$$

In many cases, the σ_Q, α_Q, $\overline{\kappa}_Q$ conductivities are not independent of each other, and obey identities connecting them at all frequencies [28]. This is the case in systems with Hamiltonians which are invariant under relativistic or Galilean transformations. However, our interest here is in systems which conserve $\boldsymbol{P}$, but do not enjoy relativistic or Galilean invariance, and such systems have not been as extensively studied. In such situations, it appears that σ_Q, α_Q, and $\overline{\kappa}_Q$ are independent response functions.

Let us now turn to the specific case of the Ising-nematic quantum critical point in two-dimensional metals [5, 6, 9]. Among the thermodynamic observables introduced above, $\mathcal{Q}$ and $\mathcal{M}$ take constant non-critical values which depend upon microscopic details. However, the entropy density, $\mathcal{S}$ does have a singular T dependence. From general scaling considerations, and allowing for violating of hyperscaling in which the spatial dimension $d \to d - \theta$, we expect [29]

$$\mathcal{S} \sim T^{(d-\theta)/z}, \tag{1.5}$$

with z the dynamic critical exponent. We can view Eq. (1.5) as the definition of the value θ. In Section IV, we will use the controlled ϵ-expansion for the Ising-nematic critical theory introduced by Dalidovich and Lee [9] to compute $\mathcal{S}$. In $d = 2$ we find the value

$$\theta = 1. \tag{1.6}$$

Roughly speaking, this violation of hyperscaling can be traced to the fact that the momentum integral along the Fermi surface is non-singular, and so only introduces an overall factor of the Fermi surface size. The single momentum dimension corresponding to this integral corresponds to the value in Eq. (1.6).

For the frequency-dependent thermoelectric conductivities, similar scaling arguments [10], followed by $d \to d - \theta$ yield

$$\sigma_Q \sim \alpha_Q \sim \frac{\overline{\kappa}_Q}{T} \sim T^{(d-2-\theta)/z}\, \Upsilon(\omega/T), \tag{1.7}$$

where Υ is a scaling function, and the three conductivities have separate scaling functions. In Sections III-E, we will use the Dalidovich-Lee ϵ expansion to compute σ_Q in the regime $\omega \gg T$ (this is the 'optical' conductivity). In this regime, and for $d = 2$, we find $\sigma_Q \sim \omega^{(d-2-\theta)/z}$, as expected from Eq. (1.7), with the value of θ again given by Eq. (1.6).

We note that we have defined the value of z by the scaling of the fermion response function transverse to the Fermi surface. The Ising-nematic critical point has $z = 3/2$ and $\theta = 1$ in $d = 2$, and so we have $\sigma_Q \sim \omega^{-2/3}$. This scaling of the optical conductivity was obtained earlier [12] for the case of a Fermi surface coupled to a U(1) gauge field, but was given a different physical interpretation [10].

We will begin in Section II by describing the action for the Ising nematic critical point. The optical conductivity will be computed in Section III, and the free energy and entropy density in Section IV.

II.   ACTION AND SCALING ANALYSIS AT TREE LEVEL

We consider a theory of fermions in $(2+1)$ dimensions which are coupled to a critical boson,

$$\begin{aligned}
S(\bar{\psi}, \psi, \Phi) = &\sum_{s=\pm}\sum_{j=1}^{N} \int \frac{d^3k}{(2\pi)^3} \tilde{\psi}^\dagger_{sj}(k)(ik_0 + sk_x + k_y^2)\tilde{\psi}_{sj}(k) \\
&+ \frac{1}{2}\int \frac{d^3k}{(2\pi)^3}(k_0^2 + k_x^2 + k_y^2)\Phi(-k)\Phi(k) \\
&+ \frac{e}{\sqrt{N}}\sum_{s=\pm}\sum_{j=1}^{N}\int \frac{d^3k}{(2\pi)^3}\int \frac{d^3q}{(2\pi)^3}\lambda_s\Phi(q)\tilde{\psi}^\dagger_{sj}(k+q)\tilde{\psi}_{sj}(k),
\end{aligned} \tag{2.1}$$

where e is the fermion-boson coupling constant, $s = \pm 1$ labels the two Fermi surface patches and λ_s equals 1 (s) for the Ising-nematic critical point (fermions coupled to a $U(1)$ gauge field). This model has been studied by many authors, including Refs. 6 and 9. In the following, we restrict ourselves to the Ising-nematic critical point and set $\lambda_s = 1$.

Introducing the spinor notation

$$\psi_j(k) = \left(\tilde{\psi}_{+,j}(k), \tilde{\psi}^\dagger_{-,j}(-k)\right)^T \qquad\qquad \bar{\psi}_j(k) = \psi^\dagger_j(k)\gamma_0 \tag{2.2}$$

with the gamma matrices $\gamma_0 = \sigma_y$ and $\gamma_x = \sigma_x$, the action can be rewritten as

$$S(\bar{\psi}, \psi, \Phi) = \sum_{j=1}^{N} \int \frac{d^3k}{(2\pi)^3} \bar{\psi}_j(k)[ik_0\gamma_0 + i(k_x + k_y^2)\gamma_x]\psi_j(k)$$

$$+ \frac{1}{2} \int \frac{d^3q}{(2\pi)^3}(q_0^2 + q_x^2 + q_y^2)\Phi(-q)\Phi(q) \qquad (2.3)$$

$$+ \frac{ie}{\sqrt{N}} \int \frac{d^3k}{(2\pi)^3} \int \frac{d^3q}{(2\pi)^3} \Phi(q)\bar{\psi}_j(k+q)\gamma_1\psi_j(k).$$

In order to obtain a controlled perturbative expansion for correlation functions, we use the dimensional regularization proposed by Dalidovich and Lee [9], which increases the codimension of the Fermi surface. The dimensionally regularized action in $(d+1)$ dimensions reads

$$S(\bar{\psi}, \psi, \Phi) = \sum_{j=1}^{N} \int \frac{d^{d+1}k}{(2\pi)^{d+1}} \bar{\psi}_j(k)[i\mathbf{\Gamma} \cdot \mathbf{K} + i\gamma_x\delta_k]\psi_j(k)$$

$$+ \frac{1}{2} \int \frac{d^{d+1}q}{(2\pi)^{d+1}}[\mathbf{Q}^2 + q_x^2 + q_y^2]\Phi(-q)\Phi(q) \qquad (2.4)$$

$$+ \frac{ie}{\sqrt{N}}\sqrt{d-1} \sum_{j=1}^{N} \int \frac{d^{d+1}k}{(2\pi)^{d+1}} \int \frac{d^{d+1}q}{(2\pi)^{d+1}} \Phi(q)\bar{\psi}_j(k+q)\gamma_x\psi_j(k),$$

where $\mathbf{K} = (k_0, k_1, \ldots, k_{d-2})$ represents frequency and $(d-2)$ components of the full $(d+1)$-dimensional energy-momentum vector. $k_1, \ldots, k_{d-2}$ are the time-like auxiliary dimensions. The gamma matrices for the new dimensions are $\mathbf{\Gamma} = (\gamma_0, \gamma_1, \ldots, \gamma_{d-2})$. We introduced the abbreviation $\delta_k = k_x + \sqrt{d-1}k_y^2$ and keep the definitions $\gamma_0 = \sigma_y$ and $\gamma_x = \sigma_x$.

Rescaling momenta as

$$\mathbf{K} = b^{-1}\mathbf{K}' \qquad\qquad k_x = b^{-1}k_x' \qquad\qquad k_y = b^{-1/2}k_y', \qquad (2.5)$$

the fermionic quadratic part of the action is invariant under rescaling for

$$\psi_j(k) = b^{d/2+3/4}\psi_j'(k'). \qquad (2.6)$$

Rescaling the bosonic fields as

$$\Phi(k) = b^{d/2+3/4}\Phi'(k') \qquad (2.7)$$

the term $\sim q_y^2$ in the bosonic quadratic part is invariant under rescaling while the terms proportional to $\mathbf{Q}^2$ and q_x^2 are irrelevant. The interaction part changes under rescaling like

$$e' = eb^{\frac{1}{2}(5/2-d)}, \qquad (2.8)$$

identifying $d = 5/2$ as the upper critical dimension. The coupling e is irrelevant for $d > 5/2$ and relevant for $d < 5/2$. This allows to access non-Fermi liquid physics perturbatively by using $\epsilon = 5/2 - d$ as expansion parameter.

Keeping only marginal terms, the ansatz for the local field theory reads

$$S(\bar{\psi}, \psi, \Phi) = \sum_{j=1}^{N} \int \frac{d^{d+1}k}{(2\pi)^{d+1}} \bar{\psi}_j(k)[i\mathbf{\Gamma} \cdot \mathbf{K} + i\gamma_x \delta_k]\psi_j(k) + \frac{1}{2} \int \frac{d^{d+1}k}{(2\pi)^{d+1}} k_y^2 \Phi(-k)\Phi(k)$$

$$+ \frac{ie\mu^{\epsilon/2}}{\sqrt{N}} \sqrt{d-1} \sum_{j=1}^{N} \int \frac{d^{d+1}k}{(2\pi)^{d+1}} \int \frac{d^{d+1}q}{(2\pi)^{d+1}} \Phi(q)\bar{\psi}_j(k+q)\psi_j(k), \tag{2.9}$$

where we introduced the momentum scale μ in order to make the coupling e dimensionless. Perturbative corrections to this action at one-loop level reintroduce dynamics for the bosonic field. The bare propagators read

$$D_0(q) = \frac{1}{q_y^2} \tag{2.10}$$

$$G_0(k) = \frac{\mathbf{\Gamma} \cdot \mathbf{K} + \gamma_x \delta_k}{i(\mathbf{K}^2 + \delta_k^2)}. \tag{2.11}$$

III. CURRENT-CURRENT CORRELATION FUNCTION AND OPTICAL CONDUCTIVITY

In this section, we compute the optical conductivity $\sigma(\omega) = \sigma_{xx}(\omega, \mathbf{q} = \mathbf{0})$ at $T = 0$ via the Kubo formula,

$$\sigma(\omega) = -\frac{1}{\Omega_m}\langle J_x J_x \rangle(i\Omega_m)|_{i\Omega_m \to \omega + i0^+}. \tag{3.1}$$

The current operator J_x is obtained by minimally coupling the action in Eq. (2.9) to a vector potential that is non-zero only in the x-direction. We obtain

$$J_x(x) = \sum_{j=1}^{N} \bar{\psi}_j(x)ie_A\gamma_x\psi_j(x) \tag{3.2}$$

where we termed the charge e_A in order to distinguish it from the coupling constant in the action.

Note that the current operator in Eq. (3.2) describes a "chiral" current. The current operator for the particle current is given by

$$J_x^N(x) = \sum_{j=1}^{N} \bar{\psi}_j(x)e_N\gamma_0\psi_j(x). \tag{3.3}$$

The chiral current is more convenient to use within codimensional regularization. In the physical dimension $d = 2$, the correlation functions for both currents are the same within the fixed point theory of Dalidovich and Lee [9]. They differ at the three-loop level [6] where both patches are coupled.

In the following sections we compute the current-current correlation function in $\mathcal{O}(\epsilon)$ and subsequently determine its scaling behaviour.
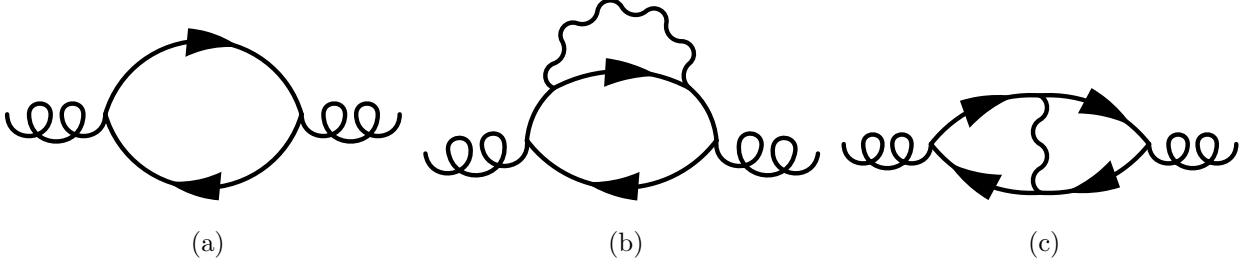
FIG. 1. Feynman diagrams for the contributions to the current-current correlation function in (a) $\mathcal{O}(N)$ and (b,c) $\mathcal{O}(1)$. The wiggly line represents the bosonic propagator and the curly line the vector potential.

A. Current-current correlation function at one-loop level

The current-current correlation function at one-loop level for $q = \omega \boldsymbol{e}_0 = \boldsymbol{Q}$ is given by a simple fermionic loop with two current insertions, as shown in Fig. 1(a),

$$
\begin{aligned}
\langle J_x J_x \rangle_{\text{1loop}}(i\omega) &= e_A^2 \sum_{j=1}^N \int \frac{d^{d+1}k}{(2\pi)^{d+1}} \, \text{tr}\big(\gamma_x G_0(k+q)\gamma_x G_0(k)\big) \\
&= -2e_A^2 N \int \frac{d^{d+1}k}{(2\pi)^{d+1}} \frac{\delta_k^2 - \boldsymbol{K}\cdot(\boldsymbol{K}+\boldsymbol{Q})}{(\boldsymbol{K}^2 + \delta_k^2)((\boldsymbol{K}+\boldsymbol{Q})^2 + \delta_k^2)}.
\end{aligned}
\tag{3.4}
$$

Evaluation as described in Appendix C 1 yields for $d = \frac{5}{2} - \epsilon$

$$
\langle J_x J_x \rangle_{\text{1loop}}(i\omega) = -e_A^2 N \int \frac{dk_y}{2\pi} u_{\text{1Loop},\epsilon=0} |\omega|^{1/2-\epsilon},
\tag{3.5}
$$

where

$$
u_{\text{1Loop},\epsilon=0} = \frac{\Gamma(\frac{5}{4})}{3\pi^{3/4}} \approx 0.128038.
\tag{3.6}
$$

For $\epsilon = 1/2$, the one-loop result is independent of frequency, as expected.

B. Two-loop self-energy correction to current-current correlation function

The self-energy correction to the current-current correlation function at two-loop level for $q = \omega \boldsymbol{e}_0 = \boldsymbol{Q}$ reads

$$
\langle J_x J_x \rangle_{\text{SE}}(i\omega) = 2e_A^2 \sum_{j=1}^N \int \frac{d^{d+1}k}{(2\pi)^{d+1}} \, \text{tr}\Big(\gamma_x G_0(k+q)\gamma_x G_0(k)\Sigma_1(k)G_0(k)\Big)
\tag{3.7}
$$

$$
= 4e^{4/3} e_A^2 \alpha_{\Sigma,d} \int \frac{d^{d+1}k}{(2\pi)^{d+1}} \Big(\frac{\mu}{|\boldsymbol{K}|}\Big)^{\frac{2\epsilon}{3}} \frac{2\delta_k^2 \boldsymbol{K}^2 + \boldsymbol{K}\cdot(\boldsymbol{K}+\boldsymbol{Q})(\delta_k^2 - \boldsymbol{K}^2)}{((\boldsymbol{K}+\boldsymbol{Q})^2 + \delta_{k+q}^2)(\boldsymbol{K}^2 + \delta_k^2)^2},
\tag{3.8}
$$

8

where $\Sigma_1(k)$ is the fermionic self-energy at one-loop level, Eq. (A12). The self-energy correction is shown diagrammatically in Fig. 1(b). This contribution contains a pole in ϵ^{-1} and evaluation as described in Appendix C 2 yields

$$\langle J_x J_x \rangle_{\text{SE}}(i\omega) = e_A^2 e^{4/3} \epsilon^{-1} \int \frac{dk_y}{(2\pi)} |\omega|^{\frac{1}{2}-\epsilon} \left(\frac{\mu}{|\omega|}\right)^{2\epsilon/3} a_{\Sigma,\epsilon=0} + \mathcal{O}(\epsilon^0), \tag{3.9}$$

where we set $\epsilon = 0$ in the numerical prefactor,

$$a_{\Sigma,\epsilon=0} = \frac{\pi^{1/4} u_{\Sigma,\epsilon=0}}{8\sqrt{2}\Gamma(\frac{7}{4})} \approx 0.0086875. \tag{3.10}$$

C. Two-loop vertex correction to current-current correlation function

The two-loop vertex correction contribution to the current-current correlation function, which is shown diagrammatically in Fig. 1(c), is given by

$$\langle J_x J_x \rangle_{\text{VC}}(i\omega) = -ie_A \sum_{j=1}^{N} \int \frac{d^{d+1}k}{(2\pi)^{d+1}} \operatorname{tr}\big(\gamma_x G_0(k+q)\Gamma_1(\boldsymbol{K}, i\omega)G_0(k)\big) \tag{3.11}$$

$$= -e_A^2 N \int \frac{d^{d+1}k}{(2\pi)^{d+1}} \frac{\operatorname{tr}\big[(\boldsymbol{\Gamma} \cdot \boldsymbol{K} + \gamma_x \delta_k)\gamma_x(\boldsymbol{\Gamma} \cdot (\boldsymbol{K} + \boldsymbol{Q}) + \gamma_x \delta_k)\gamma_x \tilde{\Gamma}_1(\boldsymbol{K}, i\omega)\big]}{(\boldsymbol{K}^2 + \delta_k^2)((\boldsymbol{K} + \boldsymbol{Q})^2 + \delta_k^2)}. \tag{3.12}$$

for $q = \omega \boldsymbol{e}_0 = \boldsymbol{Q}$. The vertex correction to the current vertex at one-loop level, $\Gamma_1(\boldsymbol{K}, \omega) = ie_A \gamma_x \tilde{\Gamma}_1(\boldsymbol{K}, \omega)$, is derived in Appendix B and given by Eq. (B6). Evaluation of Eq. (3.12) as described in Appendix C 3 yields a result that is free of poles in ϵ^{-1}. Setting $\epsilon = 0$ in the numerical prefactors, we obtain

$$\langle J_x J_x \rangle_{\text{VC}}(i\omega) = -\alpha_{\text{VC}}^{\epsilon=0} e_A^2 e^{4/3} |\omega|^{\frac{1}{2}-\epsilon} \left(\frac{\mu}{|\omega|}\right)^{2\epsilon/3} \int \frac{dk_y}{2\pi} \tag{3.13}$$

where $\alpha_{\text{VC}}^{\epsilon=0} \approx 0.0230903$.

D. Scaling behavior of optical conductivity and free energy

In this section we determine the scaling behaviour of the optical conductivity, first from general scaling arguments and subsequently for the fixed point theory for the Ising-nematic quantum-critical point using the above results for the current-current correlation function.

1. Scaling behavior of optical conductivity and free energy: General arguments

In a system with spatial dimension d, dynamical critical exponent z, $1/2 - \epsilon$ time-like auxiliary dimensions and violation of hyperscaling exponent θ, the free energy has scaling dimension

$$[F] = d - \theta + z + (1/2 - \epsilon)z = d - \theta + (3/2 - \epsilon)z. \tag{3.14}$$

The current operator is given by $J = \frac{\delta F}{\delta A}$, where A is the vector potential with scaling dimension one, and scales as $[J] = d - \theta - 1 + (3/2 - \epsilon)z$. From the Kubo formula Eq. (3.1), we obtain the scaling dimension of the optical conductivity,

$$[\sigma] = -z - (d - \theta) - (3/2 - \epsilon)z + 2[J] = d - \theta - 2 + (1/2 - \epsilon)z, \tag{3.15}$$

where we took into account that the number of spatial dimensions is effectively reduced by θ.

In $d = 2$, the free energy and optical conductivity thus scale as

$$F(T) \sim T^{(2-\theta)/z+3/2-\epsilon}, \qquad\qquad \sigma(\omega) \sim \omega^{-\theta/z+1/2-\epsilon}. \tag{3.16}$$

In the ϵ expansion, it is expected [9] that

$$z = \frac{3}{3 - 2\epsilon}. \tag{3.17}$$

In a system with the hyperscaling property and $\theta = 0$, we expect

$$F(T) \sim T^{7/2-7\epsilon/3} \tag{3.18}$$

$$\sigma(\omega) \sim \omega^{1/2-\epsilon}. \tag{3.19}$$

If hyperscaling is violated, the free energy and optical conductivity are expected to scale as

$$F(T) \sim T^{5/2-5\epsilon/3} \tag{3.20}$$

$$\sigma(\omega) \sim \omega^{-1/2-\epsilon/3} \tag{3.21}$$

for $\theta = 1$. Note that there are not expected to be any corrections to Eq. (3.20) and (3.21) at higher orders in ϵ. In a perturbative expansion in ϵ, the result for the free energy and optical conductivity would behave like

$$F(T) \sim T^{5/2-\epsilon}\big(1 - (1 - 1/z)\ln T + \ldots\big) \tag{3.22}$$

$$\sigma(\omega) \sim \omega^{-1/2-\epsilon}\big(1 + (1 - 1/z)\ln\omega + \ldots\big), \tag{3.23}$$

where $1 - 1/z = 2\epsilon/3$ for the above-mentioned fixed point theory.

2. Scaling behavior of conductivity: Evaluation for fixed point theory

The two-loop vertex correction contribution computed in Sec. III C turned out to be finite, so that only the self-energy correction yields a renormalization of the scaling-behavior of the conductivity. The current-current correlation function is thus given by

$$\langle J_x J_x\rangle(i\omega) \approx \langle J_x J_x\rangle_{\text{1Loop}}(i\omega) + \langle J_x J_x\rangle_{\text{SE}}(i\omega) + \ldots \tag{3.24}$$

$$\langle J_x J_x\rangle_{\text{1Loop}}(i\omega) = -e_A^2 N \int \frac{dk_y}{2\pi} u_{\text{1Loop},\epsilon=0} |\omega|^{1/2-\epsilon} \tag{3.25}$$

$$\langle J_x J_x\rangle_{\text{SE}}(i\omega) = e_A^2 e^{4/3} \epsilon^{-1} \int \frac{dk_y}{2\pi} |\omega|^{1/2-\epsilon} \left(\frac{\mu}{|\omega|}\right)^{2\epsilon/3} a_{\Sigma,\epsilon=0} + \ldots, \tag{3.26}$$

10

where the last line contains only the pole contribution. Resummation yields

$$\langle J_x J_x \rangle (i\omega) = -e_A^2 N \int \frac{dk_y}{2\pi} u_{1\text{Loop},\epsilon=0} |\omega|^{1/2-\epsilon} \left\{ 1 - \frac{e^{4/3}}{N\epsilon} \left(\frac{\mu}{|\omega|} \right)^{2\epsilon/3} \frac{a_{\Sigma,\epsilon=0}}{u_{1\text{Loop},\epsilon=0}} \right\} \tag{3.27}$$

$$\approx -e_A^2 N \int \frac{dk_y}{2\pi} u_{1\text{Loop},\epsilon=0} |\omega|^{1/2-\epsilon} \left\{ 1 + \gamma \ln \left(\frac{|\omega|}{\mu} \right) \right\} \tag{3.28}$$

where

$$\gamma = \frac{2}{3} \frac{e^{4/3}}{N} \frac{a_{\Sigma,\epsilon=0}}{u_{1\text{Loop},\epsilon=0}}. \tag{3.29}$$

The coupling $\frac{e^{4/3}}{N}$ is evaluated at the fixed point [9] using the β-function in $\mathcal{O}(\epsilon)$, yielding

$$\left(\frac{e^{4/3}}{N} \right)^* = u_{\Sigma,\epsilon=0}^{-1} \epsilon. \tag{3.30}$$

Inserting this result together with $u_{1\text{Loop},\epsilon=0}$ and $a_{\Sigma,\epsilon=0}$ from Eq. (3.6) and Eq. (3.10), respectively, into Eq. (3.29), we indeed obtain the value

$$\gamma = \frac{2\epsilon}{3}, \tag{3.31}$$

which is expected from Eq. (3.23) for $\theta = 1$.

E.   Pole contribution to conductivity

In Sec. I, we argued that the conductivity typically consists of a pole contribution and a "quantum" contribution σ_Q. In the results of the last sections, no pole contribution appeared. In order to understand this better, we compute the current-momentum susceptibility in the following. It is given by

$$\chi_{J_x,P_x} = \lim_{\boldsymbol{q} \to 0} \langle J_x P_x \rangle (q_0 = 0, \boldsymbol{q}). \tag{3.32}$$

At one-loop level and for $\boldsymbol{q} \neq \boldsymbol{0}$, it reads

$$\langle J_x P_x \rangle_{1\text{Loop}} (q_0 = 0, \boldsymbol{q}) = -ie_A N \int \frac{d^{d+1}k}{(2\pi)^{d+1}} \left(k_x + \frac{q_x}{2} \right) \text{tr} \left(\gamma_x G_0(k+q) \gamma_0 G_0(k) \right)$$

$$= ie_A N \int \frac{d^{d+1}k}{(2\pi)^{d+1}} \left(k_x + \frac{q_x}{2} \right) \frac{\text{tr}\{\gamma_x [\boldsymbol{\Gamma} \cdot \boldsymbol{K} + \gamma_x \delta_{k+q}] \gamma_0 [\boldsymbol{\Gamma} \cdot \boldsymbol{K} + \gamma_x \delta_k]\}}{(\boldsymbol{K}^2 + \delta_{k+q}^2)(\boldsymbol{K}^2 + \delta_k^2)} \tag{3.33}$$

where

$$P_x(x) = \frac{i}{2} \sum_{j=1}^{N} \left(\bar{\psi}_j(x) \gamma_0 \partial_x \psi_j(x) - \partial_x \bar{\psi}_j(x) \gamma_0 \psi_j(x) \right) \tag{3.34}$$

is the x-component of the momentum density operator associated with the physical time direction. Computing the trace over gamma matrices,

$$\text{tr}\{\gamma_x [\boldsymbol{\Gamma} \cdot \boldsymbol{K} + \gamma_x \delta_{k+q}] \gamma_0 [\boldsymbol{\Gamma} \cdot \boldsymbol{K} + \gamma_x \delta_k]\} = 2K_0(\delta_k + \delta_{k+q}), \tag{3.35}$$

11

and inserting the result into Eq. (3.33), it is easy to see that χ_{J_x,P_x} vanishes at one-loop level because the integrand is an odd function of K_0.

This result is also expected to hold beyond one-loop level, because the charge associated with the "chiral" current J_x measures the difference between the occupation numbers at the two opposite patches of the Fermi surface and vanishes. Moreover, in $d = 2$, J_x is equal to the fermionic density operator of the model. In that case, $\chi_{J_x,P_x} = \lim_{\boldsymbol{q}\to 0}\langle J_x P_x\rangle(q_0 = 0, \boldsymbol{q})$ is a correlation function between an operator that is odd under time reversal or spatial inversion (P_x) and one that is even under these symmetries (J_x) and thus has to vanish. The conductivity computed in the last section is thus the "quantum" contribution σ_Q.

The optical conductivity for the particle current in $d = 2$ consists of the same quantum contribution σ_Q and an additional pole contribution. The presence of the pole contribution follows from the fact that the particle current-momentum susceptibility,

$$\chi_{J^N P} = \lim_{\boldsymbol{q}\to 0}\langle J_x^N P_x\rangle(q_0 = 0, \boldsymbol{q}), \tag{3.36}$$

is non-zero in $d = 2$. This is shown in Appendix D, where we obtain

$$\langle J_x^N P_x\rangle_{1\text{Loop}}(0) = -\frac{e_N N}{\pi}\int\frac{dk_y}{(2\pi)}k_y^2. \tag{3.37}$$

at one-loop level.

IV. FREE ENERGY AT FINITE TEMPERATURE

In this section we compute the free energy at finite temperature in order to study the $T > 0$ dynamics at the Ising-nematic QCP. For this purpose we have to compute the contributions of free fermions, free bosons and a self-energy correction due to their interaction.

A. Contribution of free fermions

The contribution of free fermions is given by

$$F_{f,0}(T) - F_{f,0}(0) = -\int\frac{d^2k}{(2\pi)^2}\int\frac{d^{1/2-\epsilon}K'}{(2\pi)^{1/2-\epsilon}}\Big[T\sum_{n=\pm}\ln\big(1 + e^{-n\sqrt{\boldsymbol{K'}^2+\delta_k^2}/T}\big) - \sqrt{\boldsymbol{K'}^2 + \delta_k^2}\Big], \tag{4.1}$$

where we subtracted the result at $T = 0$ in order to make it finite. Shifting $k_x \to k_x - \sqrt{d-1}k_y^2$ and rescaling $\boldsymbol{K'} \to T\boldsymbol{K'}$, $k_x \to Tk_x$ we obtain

$$= -T^d\int\frac{d^2k}{(2\pi)^2}\int\frac{d^{1/2-\epsilon}K'}{(2\pi)^{1/2-\epsilon}}\Big[\ln\big(1 + e^{\sqrt{\boldsymbol{K'}^2+k_x^2}}\big) + \ln\big(1 + e^{-\sqrt{\boldsymbol{K'}^2+k_x^2}}\big) - \sqrt{\boldsymbol{K'}^2 + k_x^2}\Big] \tag{4.2}$$

$$= -T^{5/2-\epsilon}\int\frac{dk_y}{(2\pi)}\alpha_{f,0}, \tag{4.3}$$

where

$$\alpha_{f,0} = \frac{S_{3/2}}{(2\pi)^{3/2}} \int_0^\infty dp \sqrt{p} \left[\ln\left(1 + e^p\right) + \ln\left(1 + e^{-p}\right) - p \right] = \frac{(2\sqrt{2} - 1)\Gamma(\frac{5}{4})\zeta(\frac{5}{2})}{\sqrt{2}\pi^{5/4}} \approx 0.375866 \quad (4.4)$$

after setting $\epsilon = 0$ in the numerical prefactor.

B.   Contribution of free bosons

We compute the contribution of free bosons to the free energy for an inverse bare propagator that is quadratic in all frequency and momentum arguments and obtain

$$F_{b,0}(T) = T \int \frac{d^2q}{(2\pi)^2} \int \frac{d^{\frac{1}{2}-\epsilon}Q'}{(2\pi)^{\frac{1}{2}-\epsilon}} \ln\left(1 - e^{-\sqrt{Q'^2 + q^2}/T}\right) = -T^{7/2-\epsilon}\alpha_{b,0}. \quad (4.5)$$

In the last step we set $\epsilon = 0$ in the numerical prefactor and defined

$$\alpha_{b,0} = -\frac{S_{5/2}}{(2\pi)^{5/2}} \int_0^\infty dp\, p^{3/2} \ln\left(1 - e^{-p}\right) = \frac{3\zeta(\frac{7}{2})}{8\sqrt{2}\pi^{3/4}\Gamma(\frac{5}{4})} \approx 0.139686. \quad (4.6)$$

C.   Interaction correction to the fermionic part of the free energy

The lowest-order interaction correction to the free energy is given by

$$F_{f,b}(T) = -\frac{e^2\mu^\epsilon(d-1)}{2N} T \sum_{\Omega_m} \int \frac{d^2q}{(2\pi)^2} \int \frac{d^{\frac{1}{2}-\epsilon}Q'}{(2\pi)^{\frac{1}{2}-\epsilon}} T \sum_{\omega_n} \int \frac{d^2k}{(2\pi)^2} \int \frac{d^{\frac{1}{2}-\epsilon}K'}{(2\pi)^{\frac{1}{2}-\epsilon}} D_1(\Omega_m, \boldsymbol{Q}', \boldsymbol{q})$$
$$\times \operatorname{tr}\left[\gamma_x G_0(\omega_n + \Omega_m, \boldsymbol{K}' + \boldsymbol{Q}', \boldsymbol{k} + \boldsymbol{q})\gamma_x G_0(\omega_n, \boldsymbol{K}', \boldsymbol{k})\right], \quad (4.7)$$

where ω_n and Ω_m are fermionic and bosonic Matsubara frequencies, respectively. The corresponding Feynman diagram is shown in Fig. 2. From this expression, we need to isolate the pole contributions. In lowest order in ϵ, these are obtained by evaluating one frequency sum as an integral in the limit $T \to 0$ and the other one at finite temperature. In case the continuous frequency appears in the argument of the bosonic and a fermionic propagator, we can rewrite the diagram as a fermionic loop with an insertion of the fermionic self-energy at $T = 0$. Note that there are two such contributions. In case the continuous frequency variable appears in the two fermionic propgators, we can replace them by the bosonic self-energy at $T = 0$.

The interaction correction to the fermionic part of the free energy is then given by

$$F_{f,b}^{(1)}(T) = -\frac{e^2\mu^\epsilon(d-1)}{N} \int \frac{dQ_0}{(2\pi)} \int \frac{d^2q}{(2\pi)^2} \int \frac{d^{\frac{1}{2}-\epsilon}Q'}{(2\pi)^{\frac{1}{2}-\epsilon}} \int \frac{d^2k}{(2\pi)^2} \int \frac{d^{\frac{1}{2}-\epsilon}K'}{(2\pi)^{\frac{1}{2}-\epsilon}} T \sum_{\omega_n} D_1(Q_0, \boldsymbol{Q}', \boldsymbol{q})$$
$$\times \operatorname{tr}\left[\gamma_x G_0(\omega_n + Q_0, \boldsymbol{K}' + \boldsymbol{Q}', \boldsymbol{k} + \boldsymbol{q})\gamma_x G_0(\omega_n, \boldsymbol{K}', \boldsymbol{k})\right] \quad (4.8)$$
$$= \int \frac{d^2k}{(2\pi)^2} \int \frac{d^{\frac{1}{2}-\epsilon}K'}{(2\pi)^{\frac{1}{2}-\epsilon}} T \sum_{\omega_n} \operatorname{tr}\left[\Sigma_1(\omega_n, \boldsymbol{K}', \boldsymbol{k})G_0(\omega_n, \boldsymbol{K}', \boldsymbol{k})\right],$$
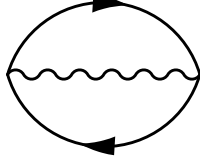
FIG. 2. Feynman diagram for the two-loop interaction correction to the free energy.

where Σ_1 is the fermionic self-energy at $T = 0$, Eq. (A12), and we included a factor of two for the two possibilities of obtaining the self-energy insertion.

After the computation of the trace over gamma matrices and a shift of $k_x \to k_x - \sqrt{d-1}k_y^2$, this contribution reads

$$
\begin{aligned}
F_{f,b}^{(1)}(T) &= -\frac{2e^{4/3}}{N}\alpha_{\Sigma,d}\mu^{2\epsilon/3}\int\frac{d^2k}{(2\pi)^2}\int\frac{d^{\frac{1}{2}-\epsilon}K'}{(2\pi)^{\frac{1}{2}-\epsilon}}T\sum_{\omega_n}\frac{1}{(\omega_n^2 + \boldsymbol{K}'^2)^{2\epsilon/6-1}(\omega_n^2 + \boldsymbol{K}'^2 + k_x^2)} \\
&= -\alpha_{f,1}\frac{e^{4/3}}{N}\int\frac{dk_y}{(2\pi)}\epsilon^{-1}\left(\frac{\mu}{T}\right)^{2\epsilon/3}T^{5/2-\epsilon},
\end{aligned}
\tag{4.9}
$$

where in the last step we computed the integrals using Feynman parameters and defined $\alpha_{f,1} = \alpha_{f,0}u_{\Sigma,0}$. Combining this result with the free fermion contribution yields

$$
\begin{aligned}
F_{f,0}(T) - F_{f,0}(0) + F_{f,b}^{(1)}(T) &= -\alpha_{f,0}\int\frac{dk_y}{(2\pi)}T^{5/2-\epsilon} - \alpha_{f,1}\frac{e^{4/3}}{N}\int\frac{dk_y}{(2\pi)}\epsilon^{-1}\left(\frac{\mu}{T}\right)^{2\epsilon/3}T^{5/2-\epsilon} \\
&= -\alpha_{f,0}\int\frac{dk_y}{(2\pi)}T^{5/2-\epsilon}\left(1 - \gamma_f\ln\frac{T}{\mu}\right),
\end{aligned}
\tag{4.10}
$$

where

$$
\gamma_f = \frac{2}{3}\frac{\alpha_{f,1}}{\alpha_{f,0}}\frac{e^{4/3}}{N}.
\tag{4.11}
$$

Evaluating γ_f at the fixed point and exploiting $(\frac{e^{4/3}}{N})^* = \frac{\epsilon}{u_{\Sigma,0}}$, we obtain $\gamma_f^* = \frac{2\epsilon}{3}$ and thus

$$
F_{f,0}(T) - F_{f,0}(0) + F_{f,b}^{(1)}(T) = -\alpha_{f,0}\int\frac{dk_y}{(2\pi)}T^{5/2-\epsilon}\left(1 - \frac{2\epsilon}{3}\ln\frac{T}{\mu}\right).
\tag{4.12}
$$

This temperature dependence is expected in this order in ϵ from Eq. (3.22) in case hyperscaling is violated with $\theta = 1$ for $d = 2$.

D. Interaction correction to the bosonic part of the free energy

In this section we evaluate the interaction correction to the bosonic part of the free energy. In order to extract the leading order contribution in ϵ, the bosonic self-energy entering the diagram as self-energy insertion and in the bosonic propagator is evaluated at $T = 0$, while the remaining

14

Matsubara frequency sum is evaluated at $T > 0$. This yields

$$
\begin{aligned}
F_{f,b}^{(2)}(T) &= -\frac{T}{2} \int \frac{d^2q}{(2\pi)^2} \int \frac{d^{\frac{1}{2}-\epsilon}Q'}{(2\pi)^{\frac{1}{2}-\epsilon}} \sum_{\Omega_m} D_1(\Omega_m, \boldsymbol{Q}', \boldsymbol{q}) \Pi(\Omega_m, \boldsymbol{Q}', \boldsymbol{q}) \\
&= \frac{T}{2} \beta_d e^2 \mu^\epsilon (d-1) \int \frac{d^2q}{(2\pi)^2} \int \frac{d^{\frac{1}{2}-\epsilon}Q'}{(2\pi)^{\frac{1}{2}-\epsilon}} \sum_{\Omega_m} \frac{\sqrt{\Omega_m^2 + \boldsymbol{Q}'^2}^{d-1}}{|q_y|^3 + \beta_d e^2 \mu^\epsilon \sqrt{\Omega_m^2 + \boldsymbol{Q}'^2}^{d-1}}.
\end{aligned}
\tag{4.13}
$$

Computing the integrals and evaluating the frequency sum using zeta-function regularization identities [10], we obtain

$$
= \frac{e^{2/3}(\beta_d \mu^\epsilon)^{1/3} S_{d-2}(d-1)}{3\sqrt{3}(2\pi)^{d-2}} T \sum_m \int \frac{dq_x}{(2\pi)} \int_0^\infty dQ Q^{d-3} \sqrt{\Omega_m^2 + Q^2}^{\frac{d-1}{3}}
\tag{4.14}
$$

$$
= \frac{\Gamma(\frac{1}{4} - \frac{\epsilon}{2})\Gamma(-\frac{1}{2} + \frac{2\epsilon}{3}) S_{d-2}(d-1)}{6\sqrt{3}\Gamma(\frac{\epsilon}{6} - \frac{1}{4})(2\pi)^{d-2}} e^{2/3}(\beta_d \mu^\epsilon)^{1/3} \int \frac{dq_x}{(2\pi)} T \sum_m \frac{1}{|\Omega_m|^{4\epsilon/3-1}}
\tag{4.15}
$$

$$
= -\frac{\pi^{5/4}(\beta_{5/2})^{1/3}}{12\sqrt{6}\Gamma(\frac{3}{4})} \int \frac{dq_x}{(2\pi)} e^{2/3} T^{2-\epsilon} \left(\frac{\mu}{T}\right)^{\epsilon/3},
\tag{4.16}
$$

where we set $\epsilon = 0$ in the numerical prefactor.

In this order of approximation, the interaction correction to the bosonic part of the free energy does not contain a pole in ϵ and the bosonic contribution to the free energy is thus not renormalized.

V. CONCLUSIONS

We have computed the optical conductivity and the free energy at the Ising-nematic quantum critical point in two-dimensional metals using the ϵ-expansion introduced by Dalidovich and Lee [9]. This method allows to study the non-Fermi liquid regime at this strongly coupled critical point in a controlled way as a stable fixed point of the renormalization group flow. We found that hyperscaling is violated with a violation of hyperscaling exponent $\theta = 1$ in $d = 2$.

The optical conductivity scales as $\sigma(\omega) \sim \omega^{-2/3}$ at the fixed point, which is close to the behaviour found in optimally doped cuprates [30]. This scaling behaviour of the optical conductivity was obtained before in Ref. [12] for a metal coupled to a $U(1)$ gauge field, but was given a different physical interpretation [10].

We also computed the free energy at finite temperature, $T > 0$. The results for the fermionic contribution to the free energy confirm violation of hyperscaling with the same exponent $\theta = 1$ in $d = 2$. At lowest order in ϵ, the bosonic contribution to the free energy was not renormalized.

In critical points without disorder, the violation of hyperscaling has previously been associated with systems above their upper-critical dimension, where the critical theory is essentially a free field theory [31]. As far as we are aware, our computation in the present paper is the first to systematically demonstrate violation of hyperscaling at a strongly-coupled fixed point. The origin

15

of the violation was the presence of a Fermi surface, and the independence of the singular terms on the momentum direction parallel to the Fermi surface. A previous computation in a system with a Fermi surface [10], which was dominated by singular contributions at hot spots on the Fermi surface, instead found that hyperscaling was preserved. We believe that with hyperscaling violation established, the path is open in similar models to understand the anomalous optical conductivity of strange metals [30].

Appendix A: One-loop self-energies

The bosonic and fermionic self-energies at one-loop level were already computed in Ref. [9]. We rederive them here for completeness. The following formulas are useful in the derivations. It is often convenient to introduce Feynman parameters via

$$\frac{1}{A^\alpha B^\beta} = \frac{\Gamma(\alpha+\beta)}{\Gamma(\alpha)\Gamma(\beta)} \int_0^1 dx \frac{x^{\alpha-1}(1-x)^{\beta-1}}{[xA+(1-x)B]^{\alpha+\beta}}. \tag{A1}$$

Traces over products of gamma matrices are evaluated using the formulas for 2×2 matrices, as we are interested in $2 \leq d < 3$,

$$\text{tr}(\gamma_i) = 0 \tag{A2}$$

$$\text{tr}(\gamma_i\gamma_j) = 2\delta_{ij} \tag{A3}$$

$$\text{tr}(\gamma_i\gamma_j\gamma_k\gamma_l) = 2(\delta_{ij}\delta_{kl} - \delta_{ik}\delta_{jl} + \delta_{il}\delta_{jk}), \tag{A4}$$

where the indices run from 0 to $d-1$.

At one-loop level, the bosonic self-energy is given by

$$\begin{aligned}
\Pi_1(q) &= \frac{e^2\mu^\epsilon}{N}(d-1) \sum_{j=1}^{N} \int \frac{d^{d+1}k}{(2\pi)^{d+1}} \text{tr}\big(\gamma_1 G_{0,j}(k+q)\gamma_1 G_{0,j}(k)\big) \\
&= -2e^2\mu^\epsilon(d-1) \int \frac{d^{d+1}k}{(2\pi)^{d+1}} \frac{\delta_{k+q}\delta_k - \boldsymbol{K}\cdot(\boldsymbol{K}+\boldsymbol{Q})}{(\boldsymbol{K}^2+\delta_k^2)((\boldsymbol{K}+\boldsymbol{Q})^2+\delta_{k+q}^2)}
\end{aligned} \tag{A5}$$
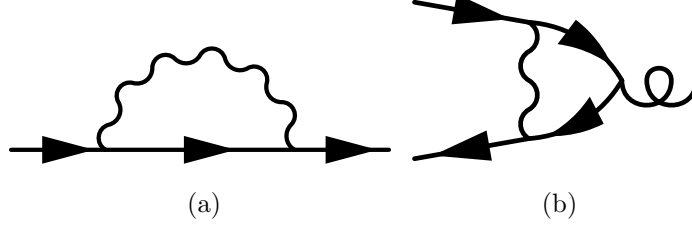
16

(a)   (b)

FIG. 3. Diagrammatic representation of the one-loop contributions to (a) the fermionic self-energy and (b) the current vertex.

where $\delta_k = k_x + \sqrt{d-1}k_y^2$. The diagrammatic represenation of this contribution is similar to Fig. 1(a), but with current vertices replaced by fermion-boson couplings. Integrating over k_x, shifting $k_y \to k_y - \frac{\delta_q}{2q_y}$ and integrating over k_y yields

$$= \frac{e^2\mu^\epsilon}{4|q_y|}\sqrt{d-1}\int\frac{d^{d-1}K}{(2\pi)^{d-1}}\left(\frac{\boldsymbol{K}\cdot(\boldsymbol{K}+\boldsymbol{Q})}{|\boldsymbol{K}||\boldsymbol{K}+\boldsymbol{Q}|}-1\right), \tag{A6}$$

where $\int\frac{d^{d-1}K}{(2\pi)^{d-1}} = \int\frac{dK_0}{2\pi}\int\frac{d^{1/2-\epsilon}K'}{(2\pi)^{1/2-\epsilon}}$ and $\boldsymbol{K} = K_0\boldsymbol{e}_0 + \boldsymbol{K}'$. The remaining integral can be computed using Feynman parameters, yielding

$$\Pi_1(q) = -\beta_d e^2 \mu^\epsilon \frac{|\boldsymbol{Q}|^{d-1}}{|q_y|}, \tag{A7}$$

where

$$\beta_d = \frac{\sqrt{d-1}\Gamma(d/2)^2}{2^d\sqrt{\pi}^{d-1}|\cos(\frac{\pi d}{2})|\Gamma(d)\Gamma(\frac{d-1}{2})}.$$

This result is the same as in Ref. 9.

The fermionic self-energy at one-loop level is given by

$$\begin{aligned}
\Sigma_1(q) &= -\frac{e^2\mu^\epsilon}{N}(d-1)\int\frac{d^{d+1}k}{(2\pi)^{d+1}}D_1(k)\gamma_x G_0(q-k)\gamma_x \\
&= \frac{ie^2\mu^\epsilon}{N}(d-1)\int\frac{d^{d+1}k}{(2\pi)^{d+1}}D_1(k)\frac{\gamma_x\delta_{q-k}-\boldsymbol{\Gamma}\cdot(\boldsymbol{Q}-\boldsymbol{K})}{(\boldsymbol{Q}-\boldsymbol{K})^2+\delta_{q-k}^2}
\end{aligned} \tag{A8}$$

where $(D_1(q))^{-1} = q_y^2 + \beta_d e^2\mu^\epsilon\frac{|\boldsymbol{Q}|^{d-1}}{|q_y|}$ is the one-loop renormalized bosonic propagator. This contribution is diagrammatically shown in Fig. 3(a). Shifting $k_x \to k_x + q_x + \sqrt{d-1}(q_y-k_y)^2$, the integrals simplify significantly because δ_{q-k} is effectively replaced by $-k_x$. After this shift, k_y appears only in the bosonic propagator, and integration over k_x and k_y yields

$$\begin{aligned}
\Sigma_1(q) &= -\frac{ie^2\mu^\epsilon}{N}(d-1)\int\frac{d^{d-1}K}{(2\pi)^{d-1}}\int_{-\infty}^{\infty}\frac{dk_y}{2\pi}\frac{|k_y|}{|k_y|^3+\beta_d e^2\mu^\epsilon|\boldsymbol{K}|^{d-1}}\int_{-\infty}^{\infty}\frac{dk_x}{2\pi}\frac{\gamma_x k_x+\boldsymbol{\Gamma}\cdot(\boldsymbol{Q}-\boldsymbol{K})}{(\boldsymbol{Q}-\boldsymbol{K})^2+k_x^2} \\
&= \frac{ie^{4/3}\mu^{2\epsilon/3}(d-1)}{3\sqrt{3}\beta_d^{1/3}N}\int\frac{d^{d-1}K}{(2\pi)^{d-1}}\frac{\boldsymbol{\Gamma}\cdot(\boldsymbol{K}-\boldsymbol{Q})}{|\boldsymbol{K}|^{\frac{d-1}{3}}|\boldsymbol{K}-\boldsymbol{Q}|}.
\end{aligned} \tag{A9}$$

17

Using Feynman parameters for computing the remaining integral, we obtain

$$\Sigma_1(q) = -i(\mathbf{\Gamma} \cdot \mathbf{Q}) \frac{e^{4/3}}{N} \left(\frac{\mu}{|\mathbf{Q}|} \right)^{2\epsilon/3} \alpha_{\Sigma,d} \tag{A10}$$

for the fermionic self-energy at one-loop level in agreement with Ref. 9, where

$$\alpha_{\Sigma,d} = \frac{(d-1)\Gamma(\frac{d-1}{3})\Gamma(\frac{d}{2})\Gamma(\frac{5-2d}{6})}{3\sqrt{3}\beta_d^{1/3}2^{d-1}\sqrt{\pi}^d\Gamma(\frac{d-1}{6})\Gamma(\frac{5d-2}{6})} \tag{A11}$$

For $d = \frac{5}{2} - \epsilon$ and $\epsilon \approx 0$, $\alpha_{\Sigma,d}$ has a pole in ϵ^{-1}. The pole contribution to the self-energy reads

$$\Sigma_1(q) = -i(\mathbf{\Gamma} \cdot \mathbf{Q}) \frac{e^{4/3}}{N} \left(\frac{\mu}{|\mathbf{Q}|} \right)^{2\epsilon/3} u_{\Sigma,\epsilon}\epsilon^{-1} + \mathcal{O}(\epsilon^0), \tag{A12}$$

where $\alpha_{\Sigma,5/2-\epsilon} \approx u_{\Sigma,\epsilon}\epsilon^{-1}$ and

$$u_{\Sigma,\epsilon} = \frac{(\frac{3}{2} - \epsilon)\Gamma(\frac{3-2\epsilon}{6})\Gamma(\frac{5-2\epsilon}{4})}{\sqrt{3}\beta_{\frac{5}{2}-\epsilon}^{1/3}2^{3/2-\epsilon}\pi^{5/4-\epsilon/2}\Gamma(\frac{3-2\epsilon}{12})\Gamma(\frac{21-10\epsilon}{12})}. \tag{A13}$$

For $\epsilon = 0$, this reduces to $u_{\Sigma,0} = \frac{\Gamma(\frac{5}{4})}{2\sqrt{3}\beta_{5/2}^{\frac{1}{3}}\pi^{\frac{7}{4}}}$.

Appendix B: Current vertex at one-loop level

In this section we derive the one-loop correction to the bare current vertex Eq. (3.2). It has been computed in Ref. 9 only for $q = 0$ and here we extend this calculation to $\omega \neq 0$.

The one-loop correction to the current vertex is shown diagrammatically in Fig. 3(b) and is given by

$$\begin{aligned}
\Gamma_1(k,q) &= -ie_A \frac{e^2\mu^\epsilon}{N} \int \frac{d^{d+1}p}{(2\pi)^{d+1}} \gamma_x G_0(k+p+q)\gamma_x G_0(k+p)\gamma_x D_1(p) \\
&= \frac{ie_A e^2\mu^\epsilon}{N} \int \frac{d^{d+1}p}{(2\pi)^{d+1}} D_1(p) \frac{1}{[(\mathbf{K}+\mathbf{P}+\mathbf{Q})^2 + \delta_{k+p+q}^2][(\mathbf{K}+\mathbf{P})^2 + \delta_{k+p}^2]} \\
&\quad \times \gamma_x[\mathbf{\Gamma} \cdot (\mathbf{K}+\mathbf{P}+\mathbf{Q}) + \gamma_x\delta_{k+p+q}]\gamma_x[\mathbf{\Gamma} \cdot (\mathbf{K}+\mathbf{P}) + \gamma_x\delta_{k+p}]\gamma_x.
\end{aligned} \tag{B1}$$

In the following we set $q = \omega\mathbf{e}_0 = \mathbf{Q}$. As $\delta_{k+p} = k_x + p_x + \sqrt{d-1}(k_y + p_y)^2$, p_y can be eliminated from the fermionic propagators by shifting $p_x \to p_x - k_x - \sqrt{d-1}(k_y + p_y)^2$, effectively reducing δ_{k+p} to p_x. Note that p_y still appears in the bosonic propagator D_1 and that the current vertex correction is only a function of $\mathbf{K}$. It then reads

$$\begin{aligned}
\Gamma_1(\mathbf{K}, i\omega) =& ie_A \frac{e^2\mu^\epsilon}{N}(d-1) \int \frac{d^{d-1}P}{(2\pi)^{d-1}} \int \frac{dp_y}{2\pi} \frac{|p_y|}{|p_y|^3 + \beta_d e^2\mu^\epsilon} \\
& \times \int \frac{dp_x}{2\pi} \frac{[-\mathbf{\Gamma} \cdot (\mathbf{K}+\mathbf{P}+\mathbf{Q}) + \gamma_x p_x][\mathbf{\Gamma} \cdot (\mathbf{K}+\mathbf{P}) + \gamma_x p_x]\gamma_x}{[(\mathbf{K}+\mathbf{P}+\mathbf{Q})^2 + p_x^2][(\mathbf{K}+\mathbf{P})^2 + p_x^2]}.
\end{aligned} \tag{B2}$$

18

For $\omega = 0$, it is easy to see that the vertex correction vanishes after exploiting properties of gamma matrices and computation of the p_x integral. Dalidovich and Lee [9] argue that this is a sufficient condition for the absence of poles in ϵ^{-1} in $\Gamma_1(\boldsymbol{K}, i\omega)$, implying the absence of poles in ϵ^{-1} in the two-loop vertex correction to the current-current correlation function. This is checked explicitly below and in Appendix C 3.

For an explicit evaluation of the one-loop vertex correction in Eq. (B2), we simplify the product in the numerator using properties of gamma matrices. All terms that are linear in p_x vanish under the integral due to symmetries. Moreover, the p_y-integral has already been solved during the computation of the fermionic self-energy. Rewriting the product in the denominators of the fermionic propgators using Feynman parameters, we obtain

$$
\begin{aligned}
\Gamma_1(\boldsymbol{K}, i\omega) = & ie_A\gamma_x \frac{(e^2\mu^\epsilon)^{2/3}}{N} \frac{2(d-1)}{3\sqrt{3}\beta_d^{1/3}} \int_0^1 dx \int \frac{d^{d-1}P}{(2\pi)^{d-1}} \int \frac{dp_x}{2\pi} \\
& \times \frac{p_x^2 - \boldsymbol{\Gamma} \cdot (\boldsymbol{K} + \boldsymbol{P} + \boldsymbol{Q})\boldsymbol{\Gamma} \cdot (\boldsymbol{K} + \boldsymbol{P})}{(\boldsymbol{P}^2)^{\frac{d-1}{6}} \left[(\boldsymbol{P} + \boldsymbol{K} + x\boldsymbol{Q})^2 + p_x^2 + x(1-x)\boldsymbol{Q}^2\right]^2}.
\end{aligned}
\tag{B3}
$$

In the next step, we perform the p_x-integration and write the result in a way that makes it transparent that the vertex correction vanishes for $\boldsymbol{Q} = 0$,

$$
\begin{aligned}
= & ie_A\gamma_x \frac{(e^2\mu^\epsilon)^{2/3}(d-1)}{6\sqrt{3}N\beta_d^{1/3}} \int_0^1 dx \int \frac{d^{d-1}P}{(2\pi)^{d-1}} \\
& \times \frac{(\boldsymbol{P} + \boldsymbol{K} + x\boldsymbol{Q})^2 + x(1-x)\boldsymbol{Q}^2 - \boldsymbol{\Gamma} \cdot (\boldsymbol{K} + \boldsymbol{P} + \boldsymbol{Q})\boldsymbol{\Gamma} \cdot (\boldsymbol{K} + \boldsymbol{P})}{(\boldsymbol{P}^2)^{\frac{d-1}{6}} \left[(\boldsymbol{P} + \boldsymbol{K} + x\boldsymbol{Q})^2 + x(1-x)\boldsymbol{Q}^2\right]^{3/2}}.
\end{aligned}
\tag{B4}
$$

The product in the denominator can further be rewritten using Feynman parameters, yielding

$$
\begin{aligned}
= & ie_A\gamma_x \frac{(e^2\mu^\epsilon)^{2/3}}{6\sqrt{3}N\beta_d^{1/3}} \frac{\Gamma(\frac{3}{2} + \frac{d-1}{6})(d-1)}{\Gamma(\frac{3}{2})\Gamma(\frac{d-1}{6})} \int_0^1 dx \int_0^1 dy \int \frac{d^{d-1}P}{(2\pi)^{d-1}} y^{\frac{d-1}{6}-1}(1-y)^{1/2} \\
& \times \frac{(\boldsymbol{P} + \boldsymbol{K} + x\boldsymbol{Q})^2 + x(1-x)\boldsymbol{Q}^2 - \boldsymbol{\Gamma} \cdot (\boldsymbol{K} + \boldsymbol{P} + \boldsymbol{Q})\boldsymbol{\Gamma} \cdot (\boldsymbol{K} + \boldsymbol{P})}{\left[(\boldsymbol{P} + (1-y)(\boldsymbol{K} + x\boldsymbol{Q}))^2 + y(1-y)(\boldsymbol{K} + x\boldsymbol{Q})^2 + x(1-x)(1-y)\boldsymbol{Q}\right]^{\frac{3}{2}+\frac{d-1}{6}}}
\end{aligned}
\tag{B5}
$$

after completing squares in the denominator. We next shift $\boldsymbol{P} \to \boldsymbol{P} - (1-y)(\boldsymbol{K} + x\boldsymbol{Q})$. Terms in the numerator that are odd in $\boldsymbol{P}$ vanish when computing the integral, and we obtain

$$
\begin{aligned}
\Gamma_1(\boldsymbol{K}, i\omega) = & ie_A\gamma_x\tilde{\Gamma}_1(\boldsymbol{K}, i\omega) \\
= & ie_A\gamma_x \frac{(e^2\mu^\epsilon)^{2/3}}{6\sqrt{3}N\beta_d^{1/3}} \frac{\Gamma(\frac{3}{2} + \frac{d-1}{6})(d-1)}{\Gamma(\frac{3}{2})\Gamma(\frac{d-1}{6})} \int_0^1 dx \int_0^1 dy \int \frac{d^{d-1}P}{(2\pi)^{d-1}} y^{\frac{d-7}{6}}(1-y)^{1/2} \\
& \times \frac{x\boldsymbol{Q} \cdot \left[(1 - 2x(1-y))\boldsymbol{Q} + 2y\boldsymbol{K}\right] - \boldsymbol{\Gamma} \cdot \boldsymbol{Q}\boldsymbol{\Gamma} \cdot (y\boldsymbol{K} - x(1-y)\boldsymbol{Q})}{\left[\boldsymbol{P}^2 + y(1-y)(\boldsymbol{K} + x\boldsymbol{Q})^2 + x(1-x)(1-y)\boldsymbol{Q}^2\right]^{\frac{3}{2}+\frac{d-1}{6}}}
\end{aligned}
\tag{B6}
$$

with $\tilde{\Gamma}_1(\boldsymbol{K}, i\omega)$ defined in an obvious way. This result is used in Appendix C 3 for the computation of the two-loop vertex correction to the current-current correlation function.

19

Appendix C: Evaluation of current-current correlation function

1. Free fermion contribution

The free fermion contribution to the current-current correlation function in Eq. (3.4) is straight-forwardly evaluated using dimensional regularization. Shifting $k_x \to k_x - \sqrt{d-1}k_y^2$, k_y disappears completely from the integrand, yielding

$$
\begin{aligned}
\langle J_x J_x \rangle_{1\text{Loop}}(i\omega) &= -2e_A^2 N \int \frac{dk_y}{2\pi} \int \frac{dk_x}{2\pi} \int \frac{d^{d-1}K}{(2\pi)^{d-1}} \frac{k_x^2 - \boldsymbol{K} \cdot (\boldsymbol{K} + \boldsymbol{Q})}{(\boldsymbol{K}^2 + k_x^2)((\boldsymbol{K} + \boldsymbol{Q})^2 + k_x^2)} \\
&= -2e_A^2 N \int \frac{dk_y}{2\pi} I_{1\text{loop}}(\boldsymbol{Q}).
\end{aligned}
\tag{C1}
$$

Introducing Feynman parameters, completing squares in the denominator and shifting $\boldsymbol{K} \to \boldsymbol{K} - (1-x)\boldsymbol{Q}$, we obtain

$$
\begin{aligned}
I_{1\text{loop}}(\boldsymbol{Q}) &= \int \frac{d^{d-1}K}{(2\pi)^{d-1}} \int \frac{dp}{(2\pi)} \int_0^1 dx \frac{p^2 - \boldsymbol{K}^2 + x(1-x)\boldsymbol{Q}^2}{[\boldsymbol{K}^2 + p^2 + x(1-x)\boldsymbol{Q}^2]^2} \\
&= \frac{\pi S_{d-1}}{(2\pi)^d} \int_0^\infty dk\, k^{d-2} \int_0^1 dx \frac{x(1-x)\boldsymbol{Q}^2}{[k^2 + x(1-x)\boldsymbol{Q}^2]^{3/2}} \\
&= \frac{S_{d-1}}{(2\pi)^d} \sqrt{\pi}\Gamma(2 - d/2) \frac{\Gamma(\frac{d-1}{2})\Gamma(d/2)^2}{\Gamma(d)} |\boldsymbol{Q}|^{d-2}.
\end{aligned}
\tag{C2}
$$

For $d = 5/2 - \epsilon$, the one-loop result for the current-current correlation function thus reads

$$
\langle J_x J_x \rangle_{1\text{loop}}(i\omega) = -e_A^2 N u_{1\text{Loop},\epsilon} \int \frac{dk_y}{2\pi} |\omega|^{1/2-\epsilon},
\tag{C3}
$$

where

$$
u_{1\text{Loop},\epsilon} = \frac{2^{\epsilon - 1/2}\Gamma(\frac{3+2\epsilon}{4})\Gamma(\frac{5-2\epsilon}{4})^2}{\sqrt{\pi}^{5/2-\epsilon}\Gamma(\frac{5-2\epsilon}{2})}.
\tag{C4}
$$

2. Self-energy correction

The two-loop self-energy correction to the current-current correlation function, Eq. (3.8), can be computed using Feynman parameters. After rewriting the integrand it reads

$$
\langle J_x J_x \rangle_{\text{SE}}(\omega) = 4(e^2 \mu^\epsilon)^{\frac{2}{3}} e_A^2 \alpha_{\Sigma,d} \int \frac{d^{d+1}k}{(2\pi)^{d+1}} \int_0^1 dx \frac{1-x}{|\boldsymbol{K}|^{\frac{2\epsilon}{3}}} \frac{2\delta_k^2 \boldsymbol{K}^2 + \boldsymbol{K} \cdot (\boldsymbol{K} + \boldsymbol{Q})(\delta_k^2 - \boldsymbol{K}^2)}{\left[x(\boldsymbol{K} + \boldsymbol{Q})^2 + (1-x)\boldsymbol{K}^2 + \delta_k^2\right]^3}.
\tag{C5}
$$

Eliminating k_y by a variable shift of k_x and subsequent integration over k_x yield

$$
\begin{aligned}
&= \frac{\Gamma(3)}{4}(e^2 \mu^\epsilon)^{\frac{2}{3}} e_A^2 \alpha_{\Sigma,d} \int \frac{dk_y}{2\pi} \int \frac{d^{d-1}K}{(2\pi)^{d-1}} \int_0^1 dx \frac{1-x}{|\boldsymbol{K}|^{\frac{2\epsilon}{3}}} \\
&\qquad \times \left[\frac{3\boldsymbol{K}^2 + \boldsymbol{K} \cdot \boldsymbol{Q}}{[\boldsymbol{K}^2 + x(2\boldsymbol{K} \cdot \boldsymbol{Q} + \boldsymbol{Q}^2)]^{\frac{3}{2}}} - \frac{3\boldsymbol{K}^2(\boldsymbol{K}^2 + \boldsymbol{K} \cdot \boldsymbol{Q})}{[\boldsymbol{K}^2 + x(2\boldsymbol{K} \cdot \boldsymbol{Q} + \boldsymbol{Q}^2)]^{\frac{5}{2}}} \right].
\end{aligned}
\tag{C6}
$$

20

Again using Feynman parameters to rewrite the products in the integrand, we obtain

$$
= \frac{\Gamma(3)}{4\Gamma(\frac{\epsilon}{3})} e_A^2 (e^2\mu^\epsilon)^{\frac{2}{3}} \alpha_{\Sigma,d} \int \frac{dk_y}{2\pi} \int \frac{d^{d-1}K}{(2\pi)^{d-1}} \int_0^1 dx \int_0^1 dy
$$
$$
\times \left[\frac{\Gamma(\frac{9+2\epsilon}{6})}{\Gamma(\frac{3}{2})} \frac{(1-x)y^{\frac{\epsilon}{3}-1}(1-y)^{\frac{1}{2}}(3\boldsymbol{K}^2 + \boldsymbol{K}\cdot\boldsymbol{Q})}{\left[\boldsymbol{K}^2 + x(1-y)(2\boldsymbol{K}\cdot\boldsymbol{Q}+\boldsymbol{Q}^2)\right]^{\frac{3}{2}+\frac{\epsilon}{3}}} \right. \tag{C7}
$$
$$
\left. - \frac{\Gamma(\frac{15+2\epsilon}{6})}{\Gamma(\frac{5}{2})} \frac{3(1-x)y^{\frac{\epsilon}{3}-1}(1-y)^{\frac{3}{2}}\boldsymbol{K}^2(\boldsymbol{K}^2+\boldsymbol{K}\cdot\boldsymbol{Q})}{\left[\boldsymbol{K}^2 + x(1-y)(2\boldsymbol{K}\cdot\boldsymbol{Q}+\boldsymbol{Q}^2)\right]^{\frac{5}{2}+\frac{\epsilon}{3}}} \right].
$$

Completing squares in the denominator as

$$
\boldsymbol{K}^2 + x(1-y)(2\boldsymbol{K}\cdot\boldsymbol{Q}+\boldsymbol{Q}^2) = (\boldsymbol{K}+x(1-y)\boldsymbol{Q})^2 + x(1-y)(1-x+xy)\boldsymbol{Q}^2, \tag{C8}
$$

shifting $\boldsymbol{K} \to \boldsymbol{K} - x(1-y)\boldsymbol{Q}$, and neglecting terms that vanish due to symmetries when performing the $\boldsymbol{K}$-integration, we obtain

$$
= \frac{\Gamma(3)}{4\Gamma(\frac{\epsilon}{3})} e_A^2 (e^2\mu^\epsilon)^{\frac{2}{3}} \alpha_{\Sigma,d} \int \frac{dk_y}{(2\pi)} \int \frac{d^{d-1}K}{(2\pi)^{d-1}} \int_0^1 dx \int_0^1 dy (1-x)y^{\frac{\epsilon}{3}-1}
$$
$$
\times \left\{ \frac{\Gamma(\frac{9+2\epsilon}{6})}{\Gamma(\frac{3}{2})} (1-y)^{\frac{1}{2}} \frac{3\boldsymbol{K}^2 - x(1-y)(1-3x(1-y))\boldsymbol{Q}^2}{\left[\boldsymbol{K}^2 + x(1-y)(1-y+xy)\boldsymbol{Q}^2\right]^{\frac{3}{2}+\frac{\epsilon}{3}}} \right. \tag{C9}
$$
$$
- \frac{\Gamma(\frac{15+2\epsilon}{6})}{\Gamma(\frac{5}{2})} \frac{3(1-y)^{\frac{3}{2}}}{\left[\boldsymbol{K}^2 + x(1-y)(1-x+xy)\boldsymbol{Q}^2\right]^{\frac{5}{2}+\frac{\epsilon}{3}}} \left[\boldsymbol{K}^4 - x(1-y)(1-2x(1-y))\boldsymbol{K}^2\boldsymbol{Q}^2 \right.
$$
$$
\left. \left. - 2x(1-y)(1-2x(1-y))(\boldsymbol{K}\cdot\boldsymbol{Q})^2 - x^3(1-y)^3(1-x(1-y))\boldsymbol{Q}^4 \right] \right\}
$$

The remaining integrals can easily be computed using `Mathematica`. First integrating over $\boldsymbol{K}$ and subsequently over x and y, the pole contribution to the two-loop self-energy correction reads

$$
\langle J_x J_x \rangle_{\mathrm{SE}}(i\omega) = \frac{\pi^{\frac{1}{4}} u_{\Sigma,\epsilon=0}}{8\sqrt{2}\Gamma(\frac{7}{4})} e_A^2 e^{4/3} \epsilon^{-1} \int \frac{dk_y}{(2\pi)} |\omega|^{\frac{1}{2}-\epsilon} \left(\frac{\mu}{|\omega|}\right)^{2\epsilon/3} + \mathcal{O}(\epsilon^0) \tag{C10}
$$

after exploiting $\alpha_{\Sigma,d} \approx u_{\Sigma,\epsilon}\epsilon^{-1}$ for $\epsilon \approx 0$ and setting ϵ to zero in the numerical prefactors.

3. Vertex correction contribution

In the following, we briefly describe the evaluation of the two-loop vertex correction contribution to the current-current correlation function, Eq. (3.12). Eliminating k_y from the integrand by shifting $k_x \to k_x - \sqrt{d-1}k_y^2$ and expanding the products of gamma matrices in the numerator, the integrand simplifies because all terms in the numerator that are odd in k_x vanish due to symmetries. We obtain

$$
\langle J_x J_x \rangle_{\mathrm{VC}}(i\omega) = -e_A^2 N \int \frac{d^{d+1}k}{(2\pi)^{d+1}} \, \mathrm{tr}\left[\frac{k_x^2 - \boldsymbol{\Gamma}\cdot\boldsymbol{K}\boldsymbol{\Gamma}\cdot(\boldsymbol{K}+\boldsymbol{Q})}{(\boldsymbol{K}^2+k_x^2)((\boldsymbol{K}+\boldsymbol{Q})^2+k_x^2)} \tilde{\Gamma}_1(\boldsymbol{K},i\omega) \right]. \tag{C11}
$$

Introduction of Feynman parameters and subsequent integration over k_x yields

$$
\begin{aligned}
= -e_A^2 N \int \frac{d^{d-1}K}{(2\pi)^{d-1}} \int \frac{dk_y}{2\pi} \int_0^1 dz \\
\times \text{tr}\left[\frac{\boldsymbol{K}^2 + (1-z)(2\boldsymbol{K}\cdot\boldsymbol{Q} + \boldsymbol{Q}^2) - \boldsymbol{\Gamma}\cdot\boldsymbol{K}\boldsymbol{\Gamma}\cdot(\boldsymbol{K}+\boldsymbol{Q})}{4\left[\boldsymbol{K}^2 + (1-z)(2\boldsymbol{K}\cdot\boldsymbol{Q}+\boldsymbol{Q}^2)\right]^{3/2}} \tilde{\Gamma}_1(\boldsymbol{K}, i\omega) \right].
\end{aligned}
\tag{C12}
$$

Inserting the one-loop correction to the current vertex in Eq. (B6), we obtain

$$
\begin{aligned}
= -e_A^2 \frac{(e^2\mu^\epsilon)^{2/3}}{24\sqrt{3}\beta_d^{1/3}} \frac{\Gamma(\frac{3}{2}+\frac{d-1}{6})(d-1)}{\Gamma(\frac{3}{2})\Gamma(\frac{d-1}{6})} \int_0^1 dx \int_0^1 dy \int_0^1 dz \int \frac{d^{d-1}K}{(2\pi)^{d-1}} \int \frac{d^{d-1}P}{(2\pi)^{d-1}} \int \frac{dk_y}{2\pi} y^{\frac{d-7}{6}}(1-y)^{1/2} \\
\times \text{tr}\left[\frac{\boldsymbol{K}^2 + (1-z)(2\boldsymbol{K}\cdot\boldsymbol{Q}+\boldsymbol{Q}^2) - \boldsymbol{\Gamma}\cdot\boldsymbol{K}\boldsymbol{\Gamma}\cdot(\boldsymbol{K}+\boldsymbol{Q})}{\left[\boldsymbol{K}^2 + (1-z)(2\boldsymbol{K}\cdot\boldsymbol{Q}+\boldsymbol{Q}^2)\right]^{3/2}} \right. \\
\left. \times \frac{x\boldsymbol{Q}\cdot\left[(1-2x(1-y))\boldsymbol{Q} + 2y\boldsymbol{K}\right] - \boldsymbol{\Gamma}\cdot\boldsymbol{Q}\boldsymbol{\Gamma}\cdot(y\boldsymbol{K} - x(1-y)\boldsymbol{Q})}{\left[\boldsymbol{P}^2 + y(1-y)(\boldsymbol{K}+x\boldsymbol{Q})^2 + x(1-x)(1-y)\boldsymbol{Q}^2\right]^{\frac{3}{2}+\frac{d-1}{6}}} \right].
\end{aligned}
\tag{C13}
$$

Again introducing Feynman parameters for the remaining product yields

$$
\begin{aligned}
= -e_A^2 \frac{(e^2\mu^\epsilon)^{2/3}}{24\sqrt{3}\beta_d^{1/3}} \frac{\Gamma(3+\frac{d-1}{6})(d-1)}{\Gamma(\frac{3}{2})^2\Gamma(\frac{d-1}{6})} \int_0^1 dw \int_0^1 dx \int_0^1 dy \int_0^1 dz \int \frac{d^{d-1}K}{(2\pi)^{d-1}} \int \frac{d^{d-1}P}{(2\pi)^{d-1}} \int_0^1 \frac{dk_y}{2\pi} \\
\times y^{\frac{d-7}{6}}(1-y)^{1/2} \text{tr}\left(\left\{ \boldsymbol{K}^2 + (1-z)(2\boldsymbol{K}\cdot\boldsymbol{Q}+\boldsymbol{Q}^2) - \boldsymbol{\Gamma}\cdot\boldsymbol{K}\boldsymbol{\Gamma}\cdot(\boldsymbol{K}+\boldsymbol{Q}) \right\} \right. \\
\left. \times \left\{ x\boldsymbol{Q}\cdot[(1-2(1-y))\boldsymbol{Q} + 2y\boldsymbol{K}] - \boldsymbol{\Gamma}\cdot\boldsymbol{Q}\boldsymbol{\Gamma}\cdot(y\boldsymbol{K} - x(1-y)\boldsymbol{Q}) \right\} \right) \\
\times w^{1/2}(1-w)^{\frac{d+2}{6}} \left[(1-w)\boldsymbol{P}^2 + [w + (1-w)y(1-y)](\boldsymbol{K}+\alpha_1\boldsymbol{Q})^2 + \alpha_2^2\boldsymbol{Q}^2 \right]^{-(3+\frac{d-1}{6})}
\end{aligned}
\tag{C14}
$$

after completion of squares in the denominator and definition of

$$
\alpha_1(w,x,y,z) = \alpha_1 = \frac{(1-w)xy(1-y) + w(1-z)}{w + (1-w)y(1-y)}
\tag{C15}
$$

$$
\begin{aligned}
\alpha_2(w,x,y,z) = \alpha_2 = \big[w(1-z) + x(1-x)(1-w)(1-z) + (1-w)x^2y(1-y) \\
- \alpha_1^2(w + (1-w)y(1-y)) \big]^{1/2}.
\end{aligned}
\tag{C16}
$$

In the next step, we shift $\boldsymbol{K} \to \boldsymbol{K} - \alpha_1\boldsymbol{Q}$ and subsequently evaluate the trace over gamma matrices. Terms in the numerator which are odd in $\boldsymbol{K}$ vanish under the integral due to symmetries. The trace over gamma matrices then yields

$$
\begin{aligned}
\text{tr}(\ldots) = 2y\boldsymbol{K}^2\boldsymbol{Q}^2 - 4y(1-x-z+2xz)(\boldsymbol{K}\cdot\boldsymbol{Q})^2 \\
+ 2\boldsymbol{Q}^4\big(1 - \alpha_1 - z(1-2\alpha_1)\big)\big(y\alpha_1 - 2x^2(1-y) + x(2-y-2y\alpha_1)\big).
\end{aligned}
\tag{C17}
$$

No contribution $\sim \boldsymbol{K}^4$ exists because the vertex correction vanishes for $|\boldsymbol{Q}| = |\omega| \to 0$.

Rescaling $\boldsymbol{K}$ and $\boldsymbol{P}$ as

$$\boldsymbol{P} \to \frac{\alpha_2}{\sqrt{1-w}}\boldsymbol{P} \qquad\qquad \boldsymbol{K} \to \frac{\alpha_2}{\sqrt{w+(1-w)y(1-y)}}\boldsymbol{K},$$

we obtain

$$\langle J_x J_x\rangle_{\mathrm{VC}}(i\omega) = -e_A^2 \frac{(e^2\mu^\epsilon)^{2/3}}{24\sqrt{3}\beta_d^{1/3}} \frac{\Gamma(3+\frac{d-1}{6})(d-1)}{\Gamma(\frac{3}{2})^2\Gamma(\frac{d-1}{6})} \int \frac{dk_y}{2\pi}$$
$$\times \left(N_{\mathrm{VC}}^{(1)}\boldsymbol{Q}^2 S_{\mathrm{VC}}^{(1)}(\boldsymbol{Q}) + N_{\mathrm{VC}}^{(2)} S_{\mathrm{VC}}^{(2)}(\boldsymbol{Q}) + N_{\mathrm{VC}}^{(3)}\boldsymbol{Q}^4 S_{\mathrm{VC}}^{(3)}(\boldsymbol{Q})\right) \tag{C18}$$

where

$$S_{\mathrm{VC}}^{(1)}(\boldsymbol{Q}) = \int\frac{d^{d-1}K}{(2\pi)^{d-1}}\int\frac{d^{d-1}P}{(2\pi)^{d-1}}\frac{\boldsymbol{K}^2}{\left[\boldsymbol{P}^2+\boldsymbol{K}^2+\boldsymbol{Q}^2\right]^{3+\frac{d-1}{6}}} = \frac{(3-2\epsilon)\Gamma(\frac{3}{4}+\frac{5\epsilon}{6})}{\Gamma(\frac{13}{4}-\frac{\epsilon}{6})2^{5-2\epsilon}\pi^{3/2-\epsilon}}(\boldsymbol{Q}^2)^{-\frac{3}{4}-\frac{5\epsilon}{6}} \tag{C19}$$

$$S_{\mathrm{VC}}^{(2)}(\boldsymbol{Q}) = \int\frac{d^{d-1}K}{(2\pi)^{d-1}}\int\frac{d^{d-1}P}{(2\pi)^{d-1}}\frac{(\boldsymbol{K}\cdot\boldsymbol{Q})^2}{\left[\boldsymbol{P}^2+\boldsymbol{K}^2+\boldsymbol{Q}^2\right]^{3+\frac{d-1}{6}}} = \frac{\Gamma(\frac{3}{4}+\frac{5\epsilon}{6})}{4^{2-\epsilon}\pi^{3/2-\epsilon}\Gamma(\frac{13}{4}-\frac{\epsilon}{6})}(\boldsymbol{Q}^2)^{\frac{1}{4}-\frac{5\epsilon}{6}} \tag{C20}$$

$$S_{\mathrm{VC}}^{(3)}(\boldsymbol{Q}) = \int\frac{d^{d-1}K}{(2\pi)^{d-1}}\int\frac{d^{d-1}P}{(2\pi)^{d-1}}\frac{1}{\left[\boldsymbol{P}^2+\boldsymbol{K}^2+\boldsymbol{Q}^2\right]^{3+\frac{d-1}{6}}} = \frac{\Gamma(\frac{7}{4}+\frac{5\epsilon}{6})}{2^{3-2\epsilon}\pi^{3/2-\epsilon}\Gamma(\frac{13}{4}-\frac{\epsilon}{6})}(\boldsymbol{Q}^2)^{-\frac{7}{4}-\frac{5\epsilon}{6}} \tag{C21}$$

$$N_{\mathrm{VC}}^{(1)} = \int_0^1 dw\int_0^1 dx\int_0^1 dy\int_0^1 dz\left(\frac{\alpha_2^2}{\sqrt{w+(1-w)y(1-y)}\sqrt{1-w}}\right)^{d-1} y^{\frac{d-7}{6}}(1-y)^{1/2}w^{1/2}$$
$$\times (1-w)^{\frac{d+2}{6}}(\alpha_2^2)^{-(3+\frac{d-1}{6})}\frac{2y\alpha_2^2}{w+(1-w)y(1-y)} \tag{C22}$$

$$N_{\mathrm{VC}}^{(2)} = \int_0^1 dw\int_0^1 dx\int_0^1 dy\int_0^1 dz\left(\frac{\alpha_2^2}{\sqrt{w+(1-w)y(1-y)}\sqrt{1-w}}\right)^{d-1} y^{\frac{d-7}{6}}(1-y)^{1/2}w^{1/2}$$
$$\times (1-w)^{\frac{d+2}{6}}(\alpha_2^2)^{-(3+\frac{d-1}{6})}\frac{-4y\alpha_2^2(1-x-z+2xz)}{w+(1-w)y(1-y)} \tag{C23}$$

$$N_{\mathrm{VC}}^{(3)} = \int_0^1 dw\int_0^1 dx\int_0^1 dy\int_0^1 dz\left(\frac{\alpha_2^2}{\sqrt{w+(1-w)y(1-y)}\sqrt{1-w}}\right)^{d-1} y^{\frac{d-7}{6}}(1-y)^{1/2}w^{1/2}$$
$$\times (1-w)^{\frac{d+2}{6}}(\alpha_2^2)^{-(3+\frac{d-1}{6})}2(1-\alpha_1-z(1-2\alpha_1))$$
$$\times (y\alpha_1 - 2x^2(1-y) + x(2-y-2y\alpha_1)). \tag{C24}$$

These integrals can easily be computed using `Mathematica`. They are free of poles in ϵ^{-1}, so that ϵ can be set to zero in numerical prefactors. This yields

$$\langle J_x J_x\rangle_{\mathrm{VC}}(i\omega) = -\alpha_{\mathrm{VC}}^{\epsilon=0} e_A^2 e^{4/3}|\omega|^{\frac{1}{2}-\epsilon}\left(\frac{\mu}{|\omega|}\right)^{2\epsilon/3}\int\frac{dk_y}{2\pi} \tag{C25}$$

where $\alpha_{\mathrm{VC}}^{\epsilon=0} \approx 0.0230903$.

23

Appendix D: Particle current-momentum susceptibility

Following the arguments in Sec. III E, we expect that the particle current-momentum suscepti-
bility is non-zero, at least in $d = 2$. It is given by

$$\chi_{J^N,P} = \lim_{\boldsymbol{q} \to 0} \langle J_x^N P_x \rangle (q_0 = 0, \boldsymbol{q}), \tag{D1}$$

where J_x^N is the x-component of the particle current. The correlation function for $\boldsymbol{q} \neq \boldsymbol{0}$ reads

$$
\begin{aligned}
\langle J_x^N P_x \rangle_{\text{1Loop}}(q_0 = 0, \boldsymbol{q}) &= -e_N N \int \frac{d^{d+1}k}{(2\pi)^{d+1}} \left(k_x + \frac{q_x}{2}\right) \text{tr}\left(\gamma_0 G_0(k+q)\gamma_0 G_0(k)\right) \\
&= e_N N \int \frac{d^{d+1}k}{(2\pi)^{d+1}} \left(k_x + \frac{q_x}{2}\right) \frac{\text{tr}\left\{\gamma_0[\boldsymbol{\Gamma} \cdot \boldsymbol{K} + \gamma_x \delta_{k+q}]\gamma_0[\boldsymbol{\Gamma} \cdot \boldsymbol{K} + \gamma_x \delta_k]\right\}}{(\boldsymbol{K}^2 + \delta_{k+q}^2)(\boldsymbol{K}^2 + \delta_k^2)}.
\end{aligned}
\tag{D2}
$$

The trace over the gamma matrices yields

$$= 2e_N N \int \frac{d^{d+1}k}{(2\pi)^{d+1}} \left(k_x + \frac{q_x}{2}\right) \frac{2K_0^2 - \boldsymbol{K}^2 - \delta_k \delta_{k+q}}{(\boldsymbol{K}^2 + \delta_{k+q}^2)(\boldsymbol{K}^2 + \delta_k^2)}. \tag{D3}$$

It is advantageous to split the physical from the auxiliary frequency directions,

$$\boldsymbol{K} = K_0 \boldsymbol{e}_0 + \boldsymbol{K}', \tag{D4}$$

in terms of which we obtain

$$= 2e_N N \int_0^1 dx \int \frac{d^{d+1}k}{(2\pi)^{d+1}} \left(k_x + \frac{q_x}{2}\right) \frac{K_0^2 - \boldsymbol{K}'^2 - \delta_k \delta_{k+q}}{(K_0^2 + \boldsymbol{K}'^2 + x\delta_k^2 + (1-x)\delta_{k+q}^2)^2} \tag{D5}$$

after introducing Feynman parameters. Shifting $k_x \to k_x - \sqrt{d-1}k_y^2$, introducing $G = q_x + \sqrt{d-1}(2k_y q_y + q_y^2)$ and completing squares in the denominator yields

$$= 2e_N N \int_0^1 dx \int \frac{d^{d+1}k}{(2\pi)^{d+1}} \frac{\left(k_x - \sqrt{d-1}k_y^2 + \frac{q_x}{2}\right)\left(K_0^2 - \boldsymbol{K}'^2 - k_x(k_x + G)\right)}{\left[K_0^2 + \boldsymbol{K}'^2 + (k_x + (1-x)G)^2 + x(1-x)G^2\right]^2}. \tag{D6}$$

After shifting $k_x \to k_x - (1-x)G$, all terms in the numerator which are odd in k_x vanish and we
obtain

$$
\begin{aligned}
= 2e_N N \int_0^1 dx \int \frac{d^{d+1}k}{(2\pi)^{d+1}} \Bigg\{ &(1-2x)G \frac{k_x^2}{[K_0^2 + \boldsymbol{K}'^2 + k_x^2 + x(1-x)G^2]^2} \\
&- \left[\sqrt{d-1}k_y^2 - \frac{q_x}{2} + (1-x)G\right] \frac{K_0^2 - \boldsymbol{K}'^2 - k_x^2 + x(1-x)G^2}{[K_0^2 + \boldsymbol{K}'^2 + k_x^2 + x(1-x)G^2]^2} \Bigg\}.
\end{aligned}
\tag{D7}
$$

It is obvious that the contribution in the first line vanishes when performing the x-integration.
Rescaling integration variables as $k_0 \to \sqrt{x(1-x)}k_0$, $k_x \to \sqrt{x(1-x)}k_x$ and $\boldsymbol{K}' \to \sqrt{x(1-x)}\boldsymbol{K}'$,
the term in the second line reads

$$
\begin{aligned}
= -2e_N N \int \frac{dk_y}{(2\pi)} \int \frac{dk_0}{(2\pi)} \int \frac{dk_x}{(2\pi)} \int \frac{d^{\frac{1}{2}-\epsilon}K'}{(2\pi)^{\frac{1}{2}-\epsilon}} \frac{K_0^2 - \boldsymbol{K}'^2 - k_x^2 + G^2}{[K_0^2 + \boldsymbol{K}'^2 + k_x^2 + G^2]^2} \\
\times \int_0^1 dx \sqrt{x(1-x)}^{d-2} \left[\sqrt{d-1}k_y^2 - \frac{q_x}{2} + (1-x)G\right]
\end{aligned}
\tag{D8}
$$

24

The remaining integrals yield

$$\int_0^1 dx \sqrt{x(1-x)}^{d-2} \left[\sqrt{d-1}k_y^2 - \frac{q_x}{2} + (1-x)G \right] = \frac{\Gamma(1+\frac{d}{2})\Gamma(\frac{d}{2})}{\Gamma(1+d)} G + \frac{\Gamma(\frac{d}{2})^2}{\Gamma(d)} \left(\sqrt{d-1}k_y^2 - \frac{q_x}{2} \right)$$

(D9)

$$\int \frac{dk_0}{(2\pi)} \int \frac{dk_x}{(2\pi)} \int \frac{d^{\frac{1}{2}-\epsilon}K'}{(2\pi)^{\frac{1}{2}-\epsilon}} \frac{K_0^2 - \boldsymbol{K'}^2 - k_x^2 + G^2}{[k_0^2 + \boldsymbol{K'}^2 + k_x^2 + G^2]^2} = \int \frac{dk_x}{(2\pi)} \int \frac{d^{\frac{1}{2}-\epsilon}K'}{(2\pi)^{\frac{1}{2}-\epsilon}} \frac{G^2}{2\sqrt{G^2 + k_x^2 + \boldsymbol{K'}^2}^3}$$

$$= \frac{1}{2\pi} \int \frac{d^{\frac{1}{2}-\epsilon}K'}{(2\pi)^{\frac{1}{2}-\epsilon}} \frac{G^2}{G^2 + \boldsymbol{K'}^2} = -\frac{|G|^{d-2}}{2^{d-1}\pi^{\frac{d}{2}-1}\sin(\frac{\pi d}{2})\Gamma(\frac{d-2}{2})}.$$

(D10)

We thus obtain

$$\langle J_x^N P_x \rangle_{1\text{Loop}}(q_0 = 0, \boldsymbol{q}) = e_N N \frac{\sqrt{d-1}\Gamma(\frac{d}{2})^2}{\pi^{\frac{d}{2}-1}\sin(\frac{\pi d}{2})\Gamma(\frac{d-2}{2})\Gamma(d)} \int \frac{dk_y}{(2\pi)} \left(k_y q_y + \frac{q_y^2}{2} + k_y^2 \right)$$

$$\times \left| \frac{q_x}{2} + \sqrt{d-1} \left(k_y q_y + \frac{q_y^2}{2} \right) \right|^{d-2}$$

(D11)

for the particle current-momentum correlation function. Note that on one-loop level the limits $d \to 2$ and $\boldsymbol{q} \to \boldsymbol{0}$ do not commute. For $d \geq 2$, we obtain

$$\lim_{d \to 2} \lim_{\boldsymbol{q} \to \boldsymbol{0}} \langle J_x^N P_x \rangle_{1\text{Loop}}(0, 0, q_y) = 0$$

(D12)

$$\lim_{\boldsymbol{q} \to \boldsymbol{0}} \lim_{d \to 2} \langle J_x^N P_x \rangle_{1\text{Loop}}(0, 0, q_y) = -\frac{e_N N}{\pi} \int \frac{dk_y}{(2\pi)} k_y^2.$$

(D13)

The result in the last line also follows from a calculation in $d = 2$.

Appendix E: One-loop conductivity at finite temperature

In this section, we compute the one-loop result for the conductivity in the limit $\omega \ll T$ for $d = 5/2 - \epsilon$. It is given by

$$\sigma_{xx}^{1\text{Loop}}(i\Omega_m) = -\frac{1}{\Omega_m} \langle J_x J_x \rangle_{1\text{Loop}}(i\Omega_m)$$

$$= \frac{2e_A^2 N}{\beta \Omega_m} \int \frac{d^2 k}{(2\pi)^2} \int \frac{d^{\frac{1}{2}-\epsilon}K'}{(2\pi)^{\frac{1}{2}-\epsilon}} \sum_n \frac{\delta_k^2 - \boldsymbol{K'}^2 - \omega_n(\omega_n + \Omega_m)}{(\omega_n^2 + \boldsymbol{K'}^2 + \delta_k^2)((\omega_n + \Omega_m)^2 + \boldsymbol{K'}^2 + \delta_k^2)},$$

(E1)

where Ω_m is a bosonic Matsubara frequency that has to be analytically continued to real frequencies, $i\Omega_m \to \omega + i\eta$, after evaluation of the sum over fermionic Matsubara frequencies ω_n.

Before summing over fermionic Matsubara frequencies, we cast this equation in a form that

makes it explicit that $\Omega_m \sigma_{xx}^{\text{1Loop}}(i\Omega_m)$ vanishes for $\Omega_m = 0$, following Ref. 32,

$$
= \frac{e_A^2 N}{\beta \Omega_m} \sum_{\omega_n} \int \frac{d^2 k}{(2\pi)^2} \int \frac{d^{\frac{1}{2}-\epsilon} K'}{(2\pi)^{\frac{1}{2}-\epsilon}} \left\{ \frac{\Omega_m^2 + 4k_x^2}{(\omega_n^2 + \boldsymbol{K}'^2 + k_x^2)\left[(\omega_n + \Omega_m)^2 + \boldsymbol{K}'^2 + k_x^2\right]} - \frac{2}{\omega_n^2 + \boldsymbol{K}'^2 + k_x^2} \right\}
$$

$$
= \frac{e_A^2 N}{\beta \Omega_m} \sum_{\omega_n} \int \frac{d^2 k}{(2\pi)^2} \int \frac{d^{\frac{1}{2}-\epsilon} K'}{(2\pi)^{\frac{1}{2}-\epsilon}} \frac{1}{\omega_n^2 + \boldsymbol{K}'^2 + k_x^2} \left\{ \frac{\Omega_m^2 + 4k_x^2}{(\omega_n + \Omega_m)^2 + \boldsymbol{K}'^2 + k_x^2} - \frac{4k_x^2}{\omega_n^2 + \boldsymbol{K}'^2 + k_x^2} \right\}. \tag{E2}
$$

Summing over the fermionic Matsubara frequencies yields

$$
= \frac{e_A^2 N}{\Omega_m} \int \frac{d^2 k}{(2\pi)^2} \int \frac{d^{\frac{1}{2}-\epsilon} K'}{(2\pi)^{\frac{1}{2}-\epsilon}} \left\{ \frac{\Omega_m^2 + 4k_x^2}{\Delta_k(\Omega_m^2 + 4\Delta_k^2)} \left[n_F(-\Delta_k) - n_F(\Delta_k) \right] \right.
$$

$$
\left. - \frac{k_x^2}{\Delta_k^3} \left[n_F(-\Delta_k) - n_F(\Delta_k) + \Delta_k \left(n_F'(\Delta_k) + n_F'(-\Delta_k) \right) \right] \right\}, \tag{E3}
$$

where $\Delta_k = \sqrt{k_x^2 + \boldsymbol{K}'^2}$. Analytical continuation using $i\Omega_m \to \omega + i\delta$ with $\delta = 0^+$ yields

$$
\sigma_{xx}^{\text{1Loop}}(\omega, T) = \frac{i e_A^2 N}{\omega + i\delta} \int \frac{d^2 k}{(2\pi)^2} \int \frac{d^{\frac{1}{2}-\epsilon} K'}{(2\pi)^{\frac{1}{2}-\epsilon}} \left\{ \frac{(-i\omega + \delta)^2 + 4k_x^2}{\Delta_k\left[(-i\omega + \delta)^2 + 4\Delta_k^2\right]} \left[n_F(-\Delta_k) - n_F(\Delta_k) \right] \right.
$$

$$
\left. - \frac{k_x^2}{\Delta_k^3} \left[n_F(-\Delta_k) - n_F(\Delta_k) + \Delta_k \left(n_F'(\Delta_k) + n_F'(-\Delta_k) \right) \right] \right\}. \tag{E4}
$$

We are interested primarily in the limit $\omega \ll T$ in order to obtain the coefficient of $\delta(\omega)$. In this case, we can set $\omega + i\delta = 0$ in the curly bracket, which yields

$$
= -\frac{i e_A^2 N}{\omega + i\delta} \int \frac{d^2 k}{(2\pi)^2} \int \frac{d^{\frac{1}{2}-\epsilon} K'}{(2\pi)^{\frac{1}{2}-\epsilon}} \frac{k_x^2}{\Delta_k^2} \left[n_F'(\Delta_k) + n_F'(-\Delta_k) \right]. \tag{E5}
$$

Taking the real part, we obtain

$$
\operatorname{Re} \sigma_{xx}^{\text{1Loop}}(\omega \ll T) = -\pi \delta(\omega) e_A^2 N \int \frac{d^2 k}{(2\pi)^2} \int \frac{d^{\frac{1}{2}-\epsilon} K'}{(2\pi)^{\frac{1}{2}-\epsilon}} \frac{k_x^2}{\Delta_k^2} \left[n_F'(\Delta_k) + n_F'(-\Delta_k) \right]
$$

$$
= 2\pi e_A^2 N \delta(\omega) T^{1/2-\epsilon} \int \frac{dk_y}{(2\pi)} \frac{\pi^{3/4-\epsilon/2}(1 - 2^{1/2+\epsilon})\Gamma(\frac{3}{2} - \epsilon)\zeta(\frac{1}{2} - \epsilon)}{(2\pi)^{3/2-\epsilon}\Gamma(\frac{7}{4} - \frac{\epsilon}{2})}. \tag{E6}
$$

For $d = 2$ ($\epsilon = 1/2$), this result reduces to

$$
\operatorname{Re} \sigma_{xx}^{\text{1Loop}}(\omega) = e_A^2 N \delta(\omega) \int \frac{dk_y}{(2\pi)}, \tag{E7}
$$

which coincides with the result that follows from Eq. (3.5).

---

[1] S. Sachdev and B. Keimer, "Quantum criticality," Physics Today **64**, 29 (2011), arXiv:1102.4628 [cond-mat.str-el].

[2] J. A. Hertz, "Quantum critical phenomena," Phys. Rev. B **14**, 1165 (1976).

[3] A. J. Millis, "Nearly antiferromagnetic fermi liquids: An analytic eliashberg approach," Phys. Rev. B **45**, 13047 (1992).

[4] A. Abanov and A. V. Chubukov, "Spin-Fermion Model near the Quantum Critical Point: One-Loop Renormalization Group Results," Phys. Rev. Lett. **84**, 5608 (2000), cond-mat/0002122.

[5] V. Oganesyan, S. A. Kivelson, and E. Fradkin, "Quantum theory of a nematic Fermi fluid," Phys. Rev. B **64**, 195109 (2001), cond-mat/0102093.

[6] M. A. Metlitski and S. Sachdev, "Quantum phase transitions of metals in two spatial dimensions. I. Ising-nematic order," Phys. Rev. B **82**, 075127 (2010), arXiv:1001.1153 [cond-mat.str-el].

[7] M. A. Metlitski and S. Sachdev, "Quantum phase transitions of metals in two spatial dimensions. II. Spin density wave order," Phys. Rev. B **82**, 075128 (2010), arXiv:1005.1288 [cond-mat.str-el].

[8] S. A. Hartnoll, D. M. Hofman, M. A. Metlitski, and S. Sachdev, "Quantum critical response at the onset of spin-density-wave order in two-dimensional metals," Phys. Rev. B **84**, 125115 (2011), arXiv:1106.0001 [cond-mat.str-el].

[9] D. Dalidovich and S.-S. Lee, "Perturbative non-Fermi liquids from dimensional regularization," Phys. Rev. B **88**, 245106 (2013), arXiv:1307.3170 [cond-mat.str-el].

[10] A. A. Patel, P. Strack, and S. Sachdev, "Hyperscaling at the spin density wave quantum critical point in two-dimensional metals," Phys. Rev. B **92**, 165105 (2015), arXiv:1507.05962 [cond-mat.str-el].

[11] P. A. Lee, "Gauge field, aharonov-bohm flux, and high-T_c superconductivity," Phys. Rev. Lett. **63**, 680 (1989).

[12] Y. B. Kim, A. Furusaki, X.-G. Wen, and P. A. Lee, "Gauge-invariant response functions of fermions coupled to a gauge field," Phys. Rev. B **50**, 17917 (1994), arXiv:cond-mat/9405083.

[13] M. Hermele, T. Senthil, M. P. A. Fisher, P. A. Lee, N. Nagaosa, and X.-G. Wen, "Stability of U (1) spin liquids in two dimensions," Phys. Rev. B **70**, 214437 (2004), cond-mat/0404751.

[14] S.-S. Lee, "Low-energy effective theory of Fermi surface coupled with U(1) gauge field in 2+1 dimensions," Phys. Rev. B **80**, 165102 (2009), arXiv:0905.4532 [cond-mat.str-el].

[15] I. Mandal and S.-S. Lee, "Ultraviolet/infrared mixing in non-Fermi liquids," Phys. Rev. B **92**, 035141 (2015), arXiv:1407.0033 [cond-mat.str-el].

[16] R. K. Kaul, M. A. Metlitski, S. Sachdev, and C. Xu, "Destruction of Néel order in the cuprates by electron doping," Phys. Rev. B **78**, 045110 (2008), arXiv:0804.1794 [cond-mat.str-el].

[17] D. Chowdhury and S. Sachdev, "Higgs criticality in a two-dimensional metal," Phys. Rev. B **91**, 115123 (2015), arXiv:1412.1086 [cond-mat.str-el].

[18] S. A. Hartnoll, R. Mahajan, M. Punk, and S. Sachdev, "Transport near the Ising-nematic quantum critical point of metals in two dimensions," Phys. Rev. B **89**, 155130 (2014), arXiv:1401.7012 [cond-mat.str-el].

[19] A. A. Patel and S. Sachdev, "DC resistivity at the onset of spin density wave order in two-dimensional

metals," Phys. Rev. B **90**, 165146 (2014), arXiv:1408.6549 [cond-mat.str-el].

[20] S. A. Hartnoll, P. K. Kovtun, M. Müller, and S. Sachdev, "Theory of the Nernst effect near quantum phase transitions in condensed matter and in dyonic black holes," Phys. Rev. B **76**, 144502 (2007), arXiv:0706.3215 [cond-mat.str-el].

[21] A. V. Andreev, S. A. Kivelson, and B. Spivak, "Hydrodynamic Description of Transport in Strongly Correlated Electron Systems," Phys. Rev. Lett. **106**, 256804 (2011), arXiv:1011.3068 [cond-mat.mes-hall].

[22] S. A. Hartnoll and D. M. Hofman, "Locally Critical Resistivities from Umklapp Scattering," Phys. Rev. Lett. **108**, 241601 (2012), arXiv:1201.3917 [hep-th].

[23] A. Lucas, S. Sachdev, and K. Schalm, "Scale-invariant hyperscaling-violating holographic theories and the resistivity of strange metals with random-field disorder," Phys. Rev. D **89**, 066018 (2014), arXiv:1401.7993 [hep-th].

[24] A. Lucas, "Conductivity of a strange metal: from holography to memory functions," JHEP **1503**, 071 (2015), arXiv:1501.05656 [hep-th].

[25] A. Lucas and S. Sachdev, "Memory matrix theory of magnetotransport in strange metals," Phys. Rev. B **91**, 195122 (2015), arXiv:1502.04704 [cond-mat.str-el].

[26] A. Lucas, J. Crossno, K. C. Fong, P. Kim, and S. Sachdev, "Transport in inhomogeneous quantum critical fluids and in the Dirac fluid in graphene," Phys. Rev. B **93**, 075426 (2016), arXiv:1510.01738 [cond-mat.str-el].

[27] R. Mahajan, M. Barkeshli, and S. A. Hartnoll, "Non-Fermi liquids and the Wiedemann-Franz law," Phys. Rev. B **88**, 125107 (2013), arXiv:1304.4249 [cond-mat.str-el].

[28] A. Lucas, S. Hartnoll, and S. Sachdev, "Holographic quantum matter," to appear (2016).

[29] L. Huijse, S. Sachdev, and B. Swingle, "Hidden Fermi surfaces in compressible states of gauge-gravity duality," Phys. Rev. B **85**, 035121 (2012), arXiv:1112.0573 [cond-mat.str-el].

[30] D. v. d. Marel, H. J. A. Molegraaf, J. Zaanen, Z. Nussinov, F. Carbone, A. Damascelli, H. Eisaki, M. Greven, P. H. Kes, and M. Li, "Quantum critical behaviour in a high-Tc superconductor," Nature **425**, 271 (2003).

[31] M. E. Fisher, M. N. Barber, and D. Jasnow, "Helicity modulus, superfluidity, and scaling in isotropic systems," Phys. Rev. A **8**, 1111 (1973).

[32] S. Sachdev, "Nonzero-temperature transport near fractional quantum Hall critical points," Phys. Rev. B **57**, 7157 (1998), arXiv:cond-mat/9709243.